



35 **Abstract**

36 Among the numerous work-related risk factors, construction workers are often exposed to  
37 awkward working postures that may lead them to develop work-related musculoskeletal disorders  
38 (WMSDs). To mitigate WMSDs among construction workers, awkward working posture  
39 recognition is the first step in proactive WMSD prevention. Several researchers have proposed  
40 wearable sensor-based systems and machine learning classifiers for awkward posture recognition.  
41 However, these wearable sensor-based systems (e.g., surface electromyography) are either  
42 intrusive or require attaching multiple sensors on workers' bodies, which may lead to workers'  
43 discomfort and systemic instability, thus, limiting their application on construction sites. In  
44 addition, machine learning classifiers are limited to human-specific shallow features which  
45 influence model performance. To address these limitations, this study proposes a novel approach  
46 by using wearable insole pressure system and recurrent neural network (RNN) models, which  
47 automate feature extraction and are widely used for sequential data classification. Therefore, the  
48 research objective is to automatically recognize and classify different types of awkward working  
49 postures in construction by using deep learning-based networks and wearable insole sensor data.  
50 The classification performance of three RNN-based deep learning models, namely: (1) long-short  
51 term memory (LSTM), (2) bidirectional LSTM (Bi-LSTM), and (3) gated recurrent units (GRU),  
52 was evaluated using plantar pressure data captured by a wearable insole system from workers on  
53 construction sites. The experimental results show that GRU model outperforms the other RNN-  
54 based deep learning models with a high accuracy of 99.01% and F1-score between 93.19% and  
55 99.39%. These results demonstrate that GRU models can be employed to learn sequential plantar  
56 pressure patterns captured by a wearable insole system to recognize and classify different types of  
57 awkward working postures. The findings of this study contribute to wearable sensor-based posture-  
58 related recognition and classification, thus, enhancing construction workers' health and safety.

59

60 **Keywords:** Awkward working postures; Deep learning networks; Wearable insole pressure  
61 system, Work-related musculoskeletal disorders, Work-related risk recognition.

62 **1. Introduction**

63 The construction industry suffers from numerous health and safety problems because construction  
64 activities involve diverse resources and physically demanding tasks. In Australia, there were 26  
65 out of 183 fatalities in the construction industry in 2019, which accounted for a 2.2 fatality rate  
66 (fatalities per 100,000 workers) across all industries (Safety Work Australia, 2020). Among  
67 construction-related health and safety problems, work-related musculoskeletal disorders (WMSDs)  
68 are the leading cause of non-fatal occupational injuries (Umer et al., 2017a; Anwer et al., 2021;  
69 Anwer et al., 2021). WMSDs refer to a wide range of injuries or disorders that result in pain and/or  
70 other sensations in the muscles, nerves, tendons, ligaments, and joints (Wang et al., 2015a).  
71 Examples of WMSDs include low back disorders, carpal tunnel syndrome, tendonitis, and bursitis  
72 (Umer et al., 2017a; Antwi-Afari et al., 2018a). According to the Health and Safety Executive  
73 (HSE) in the UK, WMSDs accounted for 57% of 81,000 work-related ill health cases injuries  
74 (HSE, 2020). Gibb et al. (2018) estimated that in the UK, WMSDs costs construction employers  
75 about GBP 650 million/year out of a total estimated burden of occupational ill-health cost of about  
76 GBP 850 million/year. Given that WMSDs still remain a health and safety problem in construction,  
77 there is an urgent need to recognize work-related risk factors that may lead workers to develop  
78 WMSDs.

79  
80 The high prevalence rate of WMSDs among construction workers could be attributed to several  
81 work-related physical risk factors, psychosocial stressors, and individual factors (Wang et al.,  
82 2015a; Umer et al., 2017b). Taken together, they can lead to work absenteeism, schedule delays,  
83 increased cost of medical expenses, loss of income and productivity, and early retirement (Umer  
84 et al., 2017a; Yu et al., 2021). Examples of work-related risk factors include repetitive motions,

85 gender, age, safety concerns, overexertion, awkward working posture, and poor working  
86 conditions such as high vibration, and extreme temperature (Wang et al., 2015a; Umer et al., 2020;  
87 Anwer et al., 2021; Yu et al., 2021). Among the various work-related risk factors, awkward  
88 working postures (e.g., stoop, squat) are the major risk factor that causes WMSDs in construction.  
89 According to the Center for Construction Research and Training (CPWR), roofers and painters are  
90 on their knees, crouching or stooping more than 60% of the time, and brick masons spend 93% of  
91 their time bending and twisting their bodies (CPWR, 2018). Consequently, research on automated  
92 recognition of awkward working postures has become relevant to both researchers and  
93 practitioners in developing proactive interventions which could aid WMSDs risk factors  
94 prevention in construction.

95  
96 Generally, one of the critical steps to mitigate WMSDs risk factors is to identify an ergonomic risk  
97 approach for recognizing a potential work-related risk factor. In the past decades, work-related  
98 risk factors were mainly recognized by using ergonomic risk approaches such as observation-based  
99 methods (McAtamney and Corlett, 1993; Hignett and McAtamney, 2000). Although these  
100 traditional ergonomic risk approaches are simple and less expensive, they mostly involve  
101 subjective judgments and a large amount of manual data which make them time-consuming, and  
102 error-prone (David, 2005). Alternatively, wearable sensing technologies have been developed to  
103 monitor and recognize work-related risk factors effectively, thus preventing WMSDs (Antwi-Afari  
104 et al., 2019a). Among them, wearable inertial measurement units (WIMUs) have been widely used  
105 for automated recognition and classification of awkward working postures among construction  
106 workers (Chen et al., 2017; Valero et al., 2017; Lee et al., 2020). WIMUs-based systems collect  
107 acceleration, angular velocity, and geomagnetic field measurements of a worker's bodily

108 movements, which are used to automatically monitor awkward working postures (Chen et al., 2017;  
109 Valero et al., 2017). However, attaching multiple WIMUs-based systems on different body parts  
110 not only significantly intrude a worker's task, but also often causes synchronization issues, body  
111 discomfort, and sensor stream deviations due to varying sensor locations (Guo et al., 2017).

112

113 In recent years, research works on automated recognition and classification of work-related risk  
114 factors have demonstrated the application of computational techniques such as machine learning  
115 classifiers to train and evaluate classifier performance (Akhavian and Behzadan, 2016; Nath et al.,  
116 2018; Ryu et al., 2019; Antwi-Afari et al., 2020a; Umer et al., 2020). Even though these studies  
117 have shown promising results, traditional machine learning classifiers implement pattern  
118 recognition approaches. These approaches require multiple pre-processing steps such as manual  
119 segmentation of continuous time-series sensor data with different window sizes, and further  
120 extraction of statistically significant feature vectors, which are inefficient and time-consuming  
121 (Portugal et al., 2018). In addition, the use of human-specific shallow features leads to poor  
122 performance in incremental learning. Moreover, traditional machine learning classifiers treat each  
123 time step of the time-series sensor data as statistically independent, thus, ignoring the temporal  
124 relationship between consecutive time steps (Rashid and Louis, 2019). These limitations of  
125 traditional machine learning classifiers motivate this current research to use deep learning  
126 networks to automatically extract relevant features with spatio-temporal dependency captured by  
127 a wearable insole pressure system.

128

129 To date, the literature mostly focuses on WIMUs-based systems and machine learning applications  
130 for automated recognition and classification of work-related risk factors. Although they provided  
131 useful evidence for mitigating WMSD risk factors among construction workers, they were limited

132 due to attaching intrusive wearable sensor-based systems and adopting machine learning classifiers  
133 that use hand-crafted feature extraction methods for model evaluation. To address these limitations,  
134 the present study proposed a non-intrusive wearable insole sensor system, which was used to  
135 collect plantar pressure data and deep learning-based networks for classification performance.  
136 Therefore, the objective of this research was to evaluate a novel approach of using deep learning-  
137 based networks and wearable insole sensor data to automatically recognize and classify different  
138 types of awkward working postures in construction. Consequently, the current study adopted  
139 recurrent neural networks (RNNs), deep learning models to train time-series plantar pressure data  
140 captured by a wearable insole pressure sensor. In this study, plantar pressure data were collected  
141 from a construction site when construction workers performed several awkward working postures  
142 (i.e., overhead working, squatting, stooping, semi-squatting, and one-legged kneeling) during their  
143 daily activities. In the context of a real construction site experiment, it was hypothesized that the  
144 proposed approach could produce reliable and better performance accuracy for classifying  
145 different types of awkward working postures. The findings of this study could not only  
146 complement existing wearable sensor-based systems used for work-related risk factors recognition  
147 but also provide a novel method that could be beneficial to both researchers and safety managers  
148 to mitigate WMSDs risk factors in construction.

149

## 150 **2. Research Background**

151 This section mainly presents existing research studies related to ergonomic risk approaches for  
152 recognizing work-related risk factors. In addition, extant literature on wearable sensor-based  
153 systems for automated recognition and WMSDs prevention are thoroughly discussed. Lastly, the

154 feasibility of using wearable insole sensor data and deep learning network-based classification in  
155 construction is discussed.

156

### 157 *2.1. Ergonomic risk approaches for recognizing work-related risk factors*

158 To mitigate the risk of developing WMSDs, several ergonomic risk recognition approaches have  
159 been developed. For instance, observational-based approaches involve manual field observations  
160 and visual inspections of work-related risk factors and workers' activities by experienced expert  
161 observers. Examples of observational-based approaches used for recording and evaluating work-  
162 related risk factors include the Ovako Working Analysis System (OWAS) (Kivi and Mattila, 1991),  
163 the Rapid Upper Limb Assessment (RULA) (McAtamney and Corlett, 1993), and Rapid Entire  
164 Body Assessment (REBA) (Hignett and McAtamney, 2000). While OWAS is designed to  
165 recognize awkward postures in workers on manufacturing lines, the RULA tool evaluates  
166 ergonomic posture risks by calculating the angles between body parts. Zhang et al. (2018)  
167 performed ergonomic posture recognition from site cameras based on OWAS. Although  
168 observational-based approaches are applied to numerous work-related risk factors, they are mostly  
169 impractical due to the substantial cost, time, subjective judgments by the experts, and technical  
170 knowledge required for post-analysis of large amounts of non-heterogeneous data (David, 2005).

171

172 Vision-based approaches consist of the use of computer-aided visual sensing technologies, such  
173 as single or multi-video cameras, stereo cameras, depth cameras, and MS Kinect, to capture human  
174 motions and recognize WMSD risk factors in construction. Ray and Teizer (2012) utilized a depth  
175 camera to detect a worker's non-ergonomic postures by modeling the worker's skeleton and  
176 measuring its joint angles. Seo et al. (2015) proposed an approach that could perform 3D

177 biomechanical analysis using visionary data from a stereo camera. While vision-based approaches  
178 are intuitive and provide reliable results, they are limited to privacy and ethical issues since  
179 cameras are generally perceived as recording devices (Yilmaz et al., 2006). In addition, with the  
180 cluttered nature of the construction industry, characterized by diverse categories of specialized  
181 resources and risk factors, and continuously changing working conditions, they may result in  
182 several technical issues such as illumination and occlusion (Chen and Shen, 2017).

183  
184 In recent years, several researchers have utilized direct measurement approaches such as wearable  
185 sensor-based systems to recognize work-related risk factors for developing WMSDs among  
186 construction workers. Examples of these approaches include surface electromyography (sEMG),  
187 electrocardiography (ECG), photoplethysmography (PPG), electrodermal activity (EDA),  
188 electroencephalogram (EEG), WIMUs-based system, and wearable insole pressure system. Umer  
189 et al. (2017b) compared the differences in lumbar biomechanics (i.e., trunk muscle activity and  
190 trunk kinematics) during three typical rebar tying postures measured by sEMG and WIMUs.  
191 Similarly, Antwi-Afari et al. (2018a) investigated the risk of developing low back disorders in  
192 rebar workers by examining muscle activity and spinal kinematics during repetitive rebar lifting  
193 tasks by using sEMG and WIMUs. Yan et al. (2017) developed a real-time motion  
194 warning personal protective equipment that enables workers' self-awareness and self-management  
195 of ergonomically hazardous operational patterns for the prevention of WMSDs based on WIMUs.  
196 By using a wearable insole pressure system, Antwi-Afari and colleagues have proposed methods  
197 to recognize awkward working postures (Antwi-Afari et al., 2018f), and recognize overexertion-  
198 related workers' activities (Antwi-Afari et al., 2020a). While previous studies have made  
199 significant contributions for automated recognition of work-related risk factors for mitigating



200 WMSDs among construction workers, they mostly utilized direct measurement approaches in a  
201 laboratory experimental setting. In this regard, whether a wearable insole pressure system would  
202 perform well on a real construction dataset remains to be evaluated in this paper.

203

## 204 *2.2. Wearable sensor-based systems for automated recognition and WMSDs prevention*

205 Monitoring and recognizing workers' activities and work-related risk factors in real-time play a  
206 significant role in evaluating workers' productivity and mitigating WMSDs risks. Consequently,  
207 automated recognition of awkward working postures is an initial step for mitigating WMSDs. With  
208 recent advancements in information technologies, wearable sensor-based systems are mostly used  
209 as ergonomic intervention tools for proactive monitoring and recognizing workers' activities.  
210 Combined with computational analyses such as machine learning classifiers, these approaches  
211 have demonstrated their feasibility in the construction domain and provided good performance  
212 evaluation for recognizing workers' activities and work-related risk factors.

213

214 Numerous wearable sensor-based systems such as global positioning system (GPS), wearable  
215 biosensors (e.g., sEMG, ECG, PPG, EEG), ultra-wideband (UWB), and radio-frequency  
216 identification (RFID) are widely used for monitoring location-based activities, physiological  
217 responses, and detecting worker-object interactions (Antwi-Afari et al., 2019a). Caldas et al. (2006)  
218 assessed the potential of using GPS sensors to improve the tracking and location of materials on  
219 construction sites. Goodrum et al. (2006) developed a tool tracking and inventory system for  
220 storing operation and maintenance data by using commercially available active RFID tags. Xing  
221 et al. (2020) explored the effects of physical fatigue on the induction of mental fatigue in  
222 construction workers in a pilot experimental method by using wearable EEG sensors. Combining

223 the efforts of previous studies in the application of location tracking and proximity detection  
224 wearable sensor-based systems within the construction environment, they all provided reliable and  
225 more robust information for enhancing and monitoring construction operations such as workers,  
226 materials, and equipment. The main limitation for applying these location tracking and proximity  
227 detection wearable sensor-based systems is the need to install tags, sensors, or markers on each  
228 individual resource, which is costly and time-consuming and thereby makes deployment on  
229 construction sites unsuitable (Teizer et al., 2007).

230  
231 To overcome these challenges, researchers and practitioners have recently adopted WIMUs-based  
232 systems for human activity recognition and work-related risk factors recognition. WIMUs-based  
233 systems consist of an accelerometer, gyroscope, and magnetometer that measure 3-axes  
234 acceleration, angular velocity, and geomagnetic field, respectively. They are smaller in size, lighter  
235 in weight, have high capacity, and provide reliable accuracy for human activity recognition and  
236 WMSDs risk prevention. In the past decades, they have been widely used in research disciplines  
237 such as rehabilitation, sports science, and healthcare, to provide multimodal interactions, support  
238 independent living in elderly people, and context-aware personalized activity assistance  
239 (Mantjarvi et al., 2001; Bao and Intille, 2004; Delrobaei et al., 2018). Mantjarvi et al. (2001)  
240 recognize human ambulation and posture based on acceleration data collected from the hip.  
241 Delrobaei et al. (2018) proposed a WIMUs-based system to quantify full-body tremor and to  
242 separate tremor-dominant from non-tremor-dominant Parkinson's Disease patients and healthy  
243 individuals. In these previous studies, they suggested that WIMU-based systems could serve as a  
244 portable ergonomic intervention tool that can be used in the home environment to monitor patients  
245 and facilitate therapeutic interventions. In the realm of construction, numerous studies have also

246 focused on human activity recognition and WMSD prevention by using WMIUs-based systems  
247 (Joshua and Varghese, 2010; Valero et al., 2017; Alwasel et al., 2017; Chen et al., 2017). Despite  
248 significant efforts, attaching multiple WIMUs-based systems on workers' bodies lead to workers'  
249 discomfort and systemic instability, thus, limiting their application on construction sites.

250  
251 To remedy this situation and considering the rapid development of microelectromechanical  
252 systems (MEMS), WIMUs-based systems have become smaller to be incorporated into smart-  
253 wearable systems such as smartphones, smartwatches, smart belts, and smart wristbands for  
254 recognizing workers' activity and work-related risk factors. Smartphones and smart wearable  
255 systems are characterized as unobtrusive because they are embedded with multiple sensor-based  
256 systems (e.g., accelerometer, gyroscope, magnetometers, barometer, light and temperature  
257 sensors), which provide a self-sufficient data collection, computing, and storage scheme. In  
258 addition, they are more intelligent, intuitive, and ubiquitous wearable systems for wireless  
259 communication networks with modern software development environments and require relatively  
260 lower maintenance and operating cost as compared to WIMUs-based systems. These approaches  
261 have been widely applied in human activity recognition and work-related risk factors classification  
262 in construction (De Dominicis et al., 2013; Akhavian and Behzadan, 2016; Nath et al., 2018; Ryu  
263 et al., 2019). De Dominicis et al. (2013) investigated the capability of smartphones for real-time  
264 data collection of geo-localization information for construction site managers. Akhavian and  
265 Behzadan (2016) presented an activity analysis framework for recognizing and classifying various  
266 construction workers' activities by using a smartphone's built-in accelerometer and gyroscope  
267 sensors. Their method used five different types of machine learning algorithms to recognize  
268 various types of construction activities. The results indicate that neural networks outperform other

269 classifiers by offering an accuracy ranging from 87% to 97% for user-dependent and 62% to 96%  
270 for user-independent categories. Nath et al. (2018) proposed a method for monitoring ergonomic  
271 risk levels caused by overexertion through body-mounted smartphones (i.e., accelerometer, linear  
272 accelerometer, and gyroscope signals). By adopting a support vector machine (SVM) classifier,  
273 the results achieved an accuracy of 90.2%. Ryu et al. (2019) examined the feasibility of the wrist-  
274 worn accelerometer-embedded activity tracker for automated action recognition during simulated  
275 masonry work in a laboratory setting. It was found that the multiclass SVM with a 4-s window  
276 size showed the best accuracy (88.1%) for classifying four different subtasks of masonry work.  
277 These machine learning classifiers have been effectively demonstrated to recognize WMSD risk  
278 factors and workers' activities, but a remaining challenge is the lack of applicable features that  
279 accurately represent the change in a worker's bodily movements caused by awkward working  
280 postures. Nevertheless, smartphones with embedded sensor-based systems by their nature are not  
281 fixed wearable sensors because of varying device locations and orientations, which can lead to  
282 data misrepresentation.

283  
284 Given the above limitations, it is still crucial to deploy other automated wearable sensing systems  
285 for activity recognition and WMSDs prevention by collecting sensing data from workers on a  
286 construction site. In addition, it would be appropriate to select computational activity models that  
287 could allow software systems to conduct reasoning algorithms to infer workers' motion or  
288 movement. To do this, the current study seeks to evaluate a novel approach by using wearable  
289 insole sensor data and deep learning-based networks to automatically recognize and classify  
290 awkward working postures in construction. The next section provides more details on its feasibility  
291 and application on construction sites.

292       2.3. *Wearable insole sensor data and deep learning-based networks for recognizing*  
293               *awkward working postures in construction*

294 Automated recognition and classification of WMSD risk factors play a crucial role in mitigating  
295 WMSDs among construction workers. It could also help researchers and safety managers to  
296 retrieve important WMSD risk factor information to facilitate their analyses and decision-making  
297 support in WMSD prevention. Previous studies have extensively focused on the application of  
298 wearable insole sensor data and machine learning classifiers for recognizing and classifying loss  
299 of balance events (Antwi-Afari et al., 2018e), awkward working postures (Antwi-Afari et al.,  
300 2018f), and overexertion related construction activities (Antwi-Afari et al., 2020a). Antwi-Afari  
301 et al. (2018f) developed a non-invasive method to recognize and classify awkward working  
302 postures based on wearable insole pressure data and machine learning classifiers. The results  
303 achieved a classification accuracy of 99.7% by using the SVM, indicating the feasibility of using  
304 a wearable insole pressure system to recognize risk factors for developing WMSDs among  
305 construction workers. However, the main limitation of traditional machine learning classifiers is  
306 the fact that they treat individual dimensions of the sensor data statistically independently. Thus,  
307 each dimension of the data is converted into feature vectors without due consideration of their  
308 spatio-temporal context. To address this limitation, the current study adopted RNN-based deep  
309 learning models, which incorporate temporal dependencies of sensor data streams and are more  
310 appropriate for monitoring work-related risk factors than considering the data stream  
311 independently. Moreover, RNN-based deep learning models provide a high level of performance  
312 for time series sequential data classification, which serves as the memory units through the gradient  
313 descent steps.

314

315 Recently, deep learning networks have received great interest from the construction-related  
316 research fields because they have achieved exceptional performance in various research topics,  
317 including image classification (Yang et al., 2018; Zhong et al., 2020), object detection and  
318 recognition (Fang et al., 2018; Fang et al., 2018), natural language processing (Zhong et al., 2020),  
319 and work-related risk factors recognition (Zhang et al., 2018; Son et al., 2019; Yu et al., 2019; Kim  
320 and Cho, 2020; Lee et al., 2020; Yang et al., 2020; Zhao and Obonyo, 2020; Seo and Lee, 2021;  
321 Wang et al., 2021; Zhao and Obonyo, 2021). Son et al. (2019) presented a method to detect  
322 construction workers under varying poses against changing backgrounds in image sequences. Yu  
323 et al. (2019) analyzed a joint-level vision-based ergonomic assessment tool for construction  
324 workers (JVEC) to provide automatic and detailed ergonomic assessments of construction workers  
325 based on construction videos. The main limitation of vision-based ergonomic assessments (i.e.,  
326 images and videos) is that they require a direct line of sight to register the movements in a  
327 construction environment (Han and Lee, 2013).

328  
329 Kim and Cho (2020) achieved a classification performance of 82.39% to 94.73% accuracy for  
330 long-short term memory (LSTM) model than conventional machine learning classifiers. Lee et al.  
331 (2020) proposed an automatic detecting technique for excessive carrying-load (DeTECLoad) to  
332 predict load-carrying weights and postures, achieving 92.46% and 96.33% performance,  
333 respectively. Yang et al. (2020) adopted a bidirectional LSTM (Bi-LSTM) algorithm for physical  
334 load detection, and they achieved 74.6 to 98.6% accuracy. Zhao and Obonyo (2021) investigated  
335 the feasibility of deploying a convolutional long short-term memory (CLN) model under  
336 incremental learning for recognizing workers' posture and achieved 87% (personalized) and 84%  
337 (generalized) recognition performance. Wang et al. (2021) developed a novel vision-based real-

338 time monitoring, evaluation, and prediction method for workers' working postures. Their method  
339 achieved 87.0% accuracy of joint point recognition and 96.0% accuracy of posture risk prediction.  
340

341 The abovementioned previous studies applied various deep learning networks for recognizing and  
342 classifying work-related risk factors such as physical loads and awkward working postures.  
343 Compared to traditional machine learning classifiers, deep learning-based networks considerably  
344 reduce the effort of choosing the right features by automatically extracting abstract features  
345 through several hidden layers, and they have been proven to work well with unsupervised learning  
346 (Seyfioğlu et al., 2018; Nguyen et al., 2019) and reinforcement learning (Ijjina and Chalavadi,  
347 2017). The major limitation of these studies which hinders their application in construction is that  
348 wearable sensing data were collected by using WIMUs. It is known that attaching multiple  
349 WIMUs-based systems on workers' bodies lead to workers' discomfort and systemic instability,  
350 thus, limiting their application on construction sites (Antwi-Afari and Li, 2018g). Knowledge from  
351 these previous studies made significant contributions to automated work-related risk factors  
352 recognition for WMSD prevention, but still, there is a need to further improve the methods to  
353 prevent WMSDs in construction workers. Even though many previous studies on deep learning-  
354 based classification have been conducted, and the fact that human activity recognition, object  
355 detection and recognition, and WMSD risk recognition have widely been studied in construction,  
356 no recent study has utilized wearable insole sensor data collected from workers on construction  
357 sites as input data for recognizing and classifying awkward working postures among construction  
358 workers. To this end, the current study employs different types of deep learning networks to  
359 recognize and classify awkward working postures based on plantar pressure data collected from a  
360 wearable insole pressure system.

### 361        **3. Research gaps, research objective, and contributions**

362        Although awkward working postures remain one of the most prevalent work-related risk factors  
363        that may lead construction workers to develop WMSDs, little research has been conducted in  
364        recognizing and classifying different types of awkward working postures among construction  
365        workers. Thus, the main research question to be answered in this study is how to combine wearable  
366        insole sensor data and deep learning-based networks for recognizing and classifying different types  
367        of awkward working postures in construction. Given the above, the present study proposed a non-  
368        intrusive wearable insole sensor system for capturing plantar pressure data, and deep learning-  
369        based networks for awkward working posture recognition and classification. Therefore, the  
370        objective of this study was to recognize and classify different types of awkward working postures  
371        by using time-series wearable insole data and deep learning-based networks.

372  
373        The main contributions of the present study can be summarized in two folds: (1) the feasibility of  
374        onsite experimental data collection for work-related risk factor recognition using a wearable insole  
375        pressure system. Numerous previous studies on work-related risk factor recognition are conducted  
376        by student participants in a controlled laboratory setting (Chen et al., 2017; Antwi-Afari et al.,  
377        2018f; Umer et al., 2020). These experimental conditions affect the generalization and validity of  
378        a given study. To improve the experimental design and data collection procedures, the present  
379        study analyzed wearable insole data collected from workers on construction sites for work-related  
380        risk factor recognition. Real time-series data collected from workers on construction sites are  
381        practically challenging due to the dynamic nature of the construction environment. Based on the  
382        field experiments, this study would provide a deeper insight towards validating the use of  
383        recognized awkward working postures performed by workers at the workplace; (2) occupational



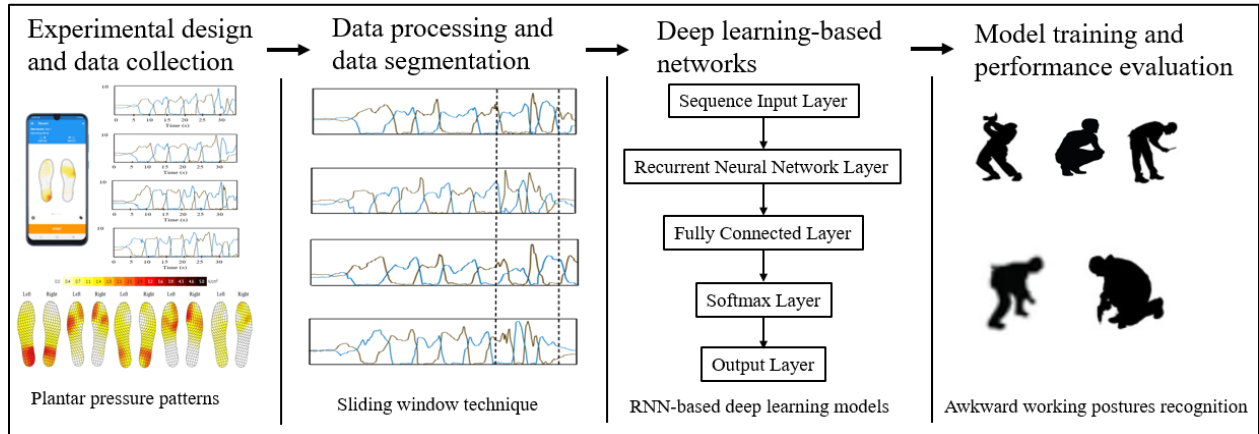
384 awkward working posture recognition and classification. In the construction domain, traditional  
385 ergonomics risk monitoring and recognition approaches (e.g., observational methods) for  
386 mitigating WMSDs are time-consuming, unreliable, and prone to errors. The proposed work-  
387 related risk factor recognition uses time-series wearable insole data (i.e., plantar pressure patterns)  
388 and RNN-based deep learning models (e.g., LSTM, Bi-LSTM, and gated recurrent units (GRU))  
389 for recognizing and classifying awkward working postures in construction. With this approach,  
390 workers' awkward working postures could be automatically monitored throughout the course of  
391 their work without any expert's interference or observation. In addition, this present study will add  
392 to the extant literature in this domain by utilizing both time series wearable insole sensor data and  
393 deep learning networks for practical application on construction sites. By adopting deep learning  
394 models, wearable insole data will be automatically extracted with highly representative features,  
395 containing spatio-temporal of plantar pressure patterns. Notably, this helps to enrich wearable  
396 sensor pattern data derived purely from time-series data for computational analysis and reasoning.  
397 Consequently, this proposed approach could enhance the generality and automation in construction  
398 safety management, especially for WMSD prevention.

399

#### 400 **4. Research methods**

401 This section discusses the experimental design and data collection procedures such as recruiting  
402 participants, experimental apparatus (i.e., wearable insole pressure system), and field experiment,  
403 and plantar pressure data collection from rebar workers on construction site. It also explains the  
404 data processing and data segmentation approach by adopting the sliding window technique. Next,  
405 three RNN-based deep learning models were adopted and discussed. The final stage is model  
406 training and performance evaluation, where each RNN-based deep learning model was trained by

407 using plantar pressure patterns as input data and the performance of the trained models was  
 408 evaluated using metrics. Fig. 1 illustrates the framework of the proposed approach. Further details  
 409 are presented below.



410  
 411 **Fig. 1.** A framework of the proposed approach

412

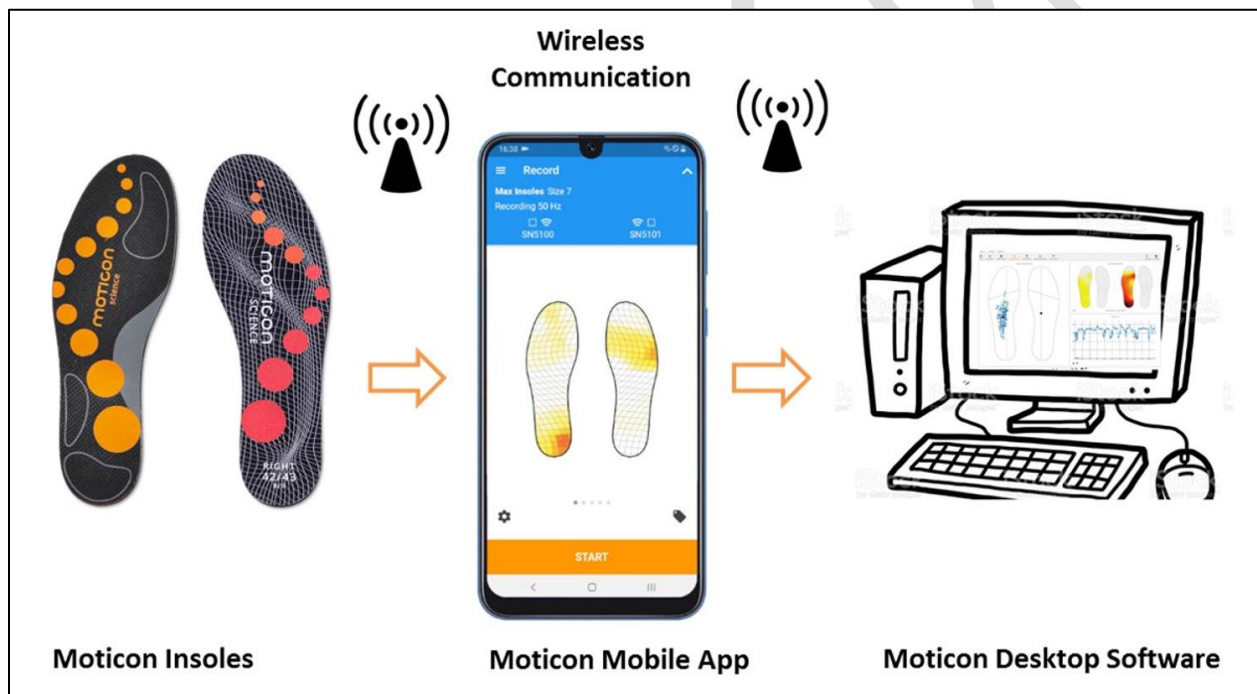
413 *4.1. Experimental design and data collection*

414 *4.1.1. Participants*

415 Ten male participants (i.e., construction rebar workers) were voluntarily recruited to participate in  
 416 the experiments. Construction rebar workers were recruited and participated in this study because  
 417 repetitive rebar tasks (e.g., preparing and assembling rebars) are physically demanding and often  
 418 involve long working hours, awkward working postures, and manual lifting activities (Buchholz  
 419 et al., 2003; Anwer et al., 2021). The participants mean age, weight, height, and shoe size were  $38$   
 420  $\pm 1.82$  years,  $76 \pm 2.79$  kg,  $1.75 \pm 0.32$  m, and  $10.32 \pm 1.03$  EU size, respectively. All participants  
 421 had no history of (1) significant foot injuries or lower extremity abnormalities during the last 12  
 422 months preceding the start of the study, and (2) neurological conditions or disabilities or other  
 423 conditions that affected fall and/or balance. The experimental protocol for data collection was  
 424 reviewed and approved by the Institutional Review Board. In addition, a written consent was  
 425 obtained from each participant after a verbal explanation of the experimental procedures.

426 4.1.2. *Experimental apparatus*

427 An OpenGo system (Moticon GmbH, Munich, Germany), which is a wearable insole pressure  
428 system for measuring plantar pressure distribution was used in the current study. Each left or right  
429 wearable sensor insole contains 16 capacitive pressure sensors, a 3-axis gyroscope (MEMS  
430 LSM6DSL, ST Microelectronics), and a 3-axis accelerometer. A sampling frequency of 50Hz was  
431 used for data collection. Further details of this wearable insole pressure system are presented in  
432 related studies (Antwi-Afari and Li, 2018g; Antwi-Afari et al., 2018e; Antwi-Afari et al., 2018f).  
433 Fig. 2 shows the overview of the mobile application user interface of the wearable insole system.



434 **Fig. 2.** Overview of the mobile application user interface of the wearable insole system  
435

436 4.1.3. *Field experiment and data collection*

438 Data collection was conducted on a construction site. Participants wore a safety boot with an  
439 inserted wearable insole. Each participant was studied during daily repetitive rebar tasks such as  
440 lifting, carrying, cutting, or tying rebars. While the participants performed their daily workplace  
441 activities, only five different types of awkward working postures were observed and collected.

442 They mainly included overhead working, squatting, stooping, semi-squatting, and one-legged  
443 kneeling. These awkward working postures were studied because they are often used in repetitive  
444 rebar tasks and expose rebar workers to high risk of developing WMSDs (Umer et al., 2017b;  
445 Antwi-Afari et al., 2018a). Fig. 3 depicts the field experimental trials of different types of awkward  
446 working postures. In the overhead working posture, participants were captured in an upright stance  
447 while working with their hands touching a bar above their head (Fig. 3a). Squat posture was  
448 identified when the participants maintained a full squat (Fig. 3b). Stoop posture involved full trunk  
449 flexion with bilateral knee extension in standing (Fig. 3c). Semi-squat posture involved bilateral  
450 knee bending (Fig. 3d). Lastly, one-legged kneeling was seen when the participants bent either of  
451 their knees to work in a kneeling position (Fig. 3e). Each participant performed a total of 75  
452 experimental tasks, consisting of 5 types of awkward working postures and 15 repeated  
453 experimental trials. Each experimental trial lasted for 30 seconds. Before field data collection, all  
454 participants were given sufficient time to familiarize themselves with the experimental apparatus  
455 (i.e., wearable insole pressure system) to eliminate systematic bias. The participants were also  
456 given enough rest (approx. 5 mins) between successive experimental trials to prevent injuries and  
457 physical fatigue. Notably, all experimental trials were conducted in an outdoor construction  
458 environment under natural conditions. The participants' plantar pressure data were synchronized  
459 and recorded by using a video camera for all experimental tasks. In this study, awkward working  
460 postures were defined as postures that deviated significantly from the neutral position and might  
461 cause WMSDs after being sustained for a long time (Karwowski, 2001). Moreover, it is worth  
462 mentioning that these awkward working postures exceeded the internationally recommended trunk  
463 inclination for the angles of various body parts for static working postures as defined by the  
464 International Organization for Standardization (ISO 11226:2000) (ISO, 2006).



465  
466 **Fig. 3.** Field experiments of different types of awkward working postures: (a) Overhead working;  
467 (b) Squatting; (c) Stooping; (d) Semi-squatting; and (e) One-legged kneeling

468

#### 469 *4.2. Data processing and data segmentation*

470 After data collection, the next stage is data processing and data segmentation. The collected data  
471 were stored in the mobile phone, and they were wirelessly transferred onto a desktop computer for  
472 data processing. For each observed awkward working posture, the participants performed 15  
473 repeated trials. It is worth noting that the wearable insole pressure system can capture plantar  
474 pressure patterns, acceleration, angular velocity, ground reaction force, and center of pressure data.  
475 However, all the collected data except plantar pressure patterns data were removed from the dataset  
476 during data processing. As such, only plantar pressure patterns were labelled and used for data  
477 segmentation. Class labelling was conducted by using the recorded videos and the collected plantar  
478 pressure data. The signals were visually inspected for noise or signal artefacts. Since plantar  
479 pressure patterns were evenly distributed and didn't cause any unrelated changes to different types  
480 of awkward working postures, no further signal artefacts were conducted during data processing.  
481 In the data segmentation stage, a sliding window technique was adopted to divide plantar pressure  
482 data into smaller segments, each segment containing a specified number of data samples (Preece  
483 et al., 2009). The purpose of this stage is to obtain labeled segments from the continuous stream

484 of wearable insole data to evaluate the performance of the deep learning networks. Since the  
485 sampling frequency for data collection was 50 Hz, 50 data samples are obtained every second for  
486 data processing. Given the experimental conditions, the dataset contains 10 participants with  
487 1,125,000 data samples of five classes. By considering the conducted experiments which involved  
488 repetitive rebar tasks, a window size of 5.12 s, which represents 256 ( $2^8$ ) was suitable for dividing  
489 plantar pressure data into smaller segments. This window size data segment was chosen by initially  
490 analyzing the collected plantar pressure data to include representative awkward working postures  
491 in order to optimize the recognition performance. To prevent missing relevant data, an overlapping  
492 of consecutive windows was conducted. A 50% overlap of adjacent data segment lengths was used  
493 as demonstrated in previous studies (Antwi-Afari et al., 2018e; Antwi-Afari et al., 2018f).

494

#### 495 *4.3. Deep learning-based networks*

##### 496 *4.3.1. Recurrent neural network (RNN) model architectures*

497 RNN is a subset of deep learning-based networks on the principle of extracting the output layer  
498 and feeding it back as the input of another layer to predict the output of the current layer (Inoue et  
499 al., 2018). Fig. 4 represents an overview of the RNN model architecture. As shown in Fig. 4a, the  
500 basic architecture of an RNN consists of an input, output, activation function, and a recurrent loop.  
501 Fig. 4b illustrates the structure of an unfolded RNN into a full network that allows it to perform a  
502 sequence of input data. Generally, RNN model receives the input  $x_0$  from the sequence of input  
503 data, performs some calculations resulting in  $h_0$ , which, together with  $x_1$ , compose the input to the  
504 next step. Similarly, the output  $h_1$  with the input  $x_2$  will be the input to the next step, and so on. It  
505 is worth noting that  $y_t$  is the same as  $h_t$ .

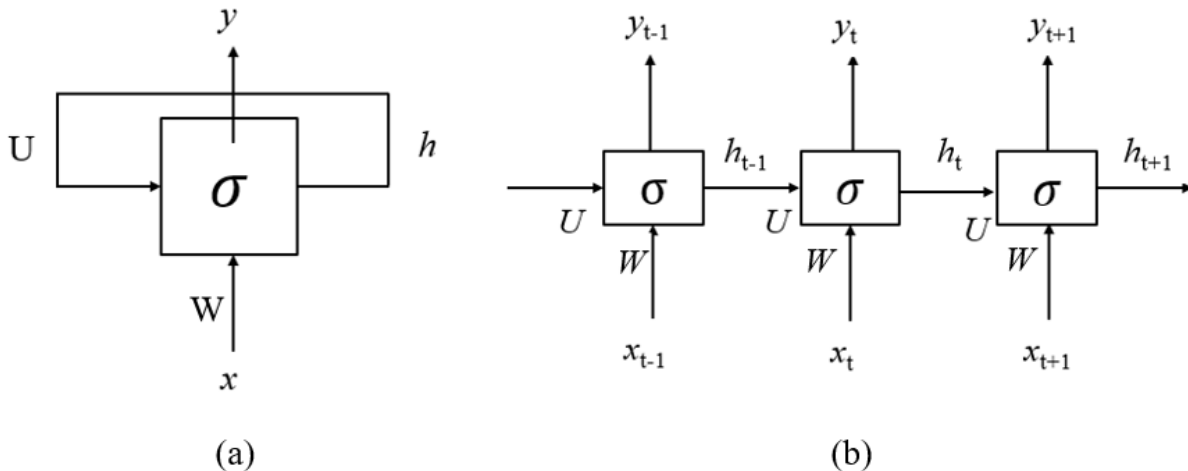
506

507 The value of  $h_t$  is calculated using Equation 1. As illustrated in Equation 1, the input  $x_t$  is modified  
 508 by  $W$  and  $h_{t-1}$  is modified by  $U$ .

$$509 \quad h_t = \sigma(Wx_t + Uh_{t-1}) \quad (1)$$

510 Where,  $x_t$  represents the input of the structure at time step  $t$ ,  $h_t$ , is the output of the structure at time  
 511 step  $t$ ,  $W$  is the weight matrix of the input to the hidden layer at time  $t$ ,  $U$  is the weight matrix of  
 512 the hidden layer at time  $t-1$ , and  $\sigma$  represents the activation function.

513  
 514 Like other neural network structures, RNN models learn weights ( $W, U$ ) through training using  
 515 the backpropagation technique. The network then determines the accuracy of the model by using  
 516 an error function (loss function) and calculating the derivatives of the loss function with respect to  
 517 the weight. In addition, the network uses an activation function to simplify the mathematical  
 518 calculations related to the application of backpropagation. In the following section, this study  
 519 presents three types of RNN-based deep learning models that were used for classifying different  
 520 types of awkward working postures.



521  
 522 **Fig. 4.** An overview of the RNN model architecture: (a) The basic architecture of an RNN; and (b)

523 The structure of an unfolded RNN

524 4.3.1.1. Long-short term memory (LSTM)

525 LSTM is a type of RNN model with an enhanced function to calculate hidden states. Hochreiter  
526 and Schmidhuber (1997) proposed LSTM network to solve temporal sequences and long-term  
527 dependency problems by adding the gating mechanism. Compared to traditional RNN models,  
528 LSTM network can solve the vanishing and exploding gradient problems because it extends RNN  
529 with memory cells which can ease the learning of temporal relationships on long time scales.

530

531 Fig. 5 shows LSTM cell architecture. This cell determines which data to keep in memory and  
532 which data to ignore using the concept of gating. LSTM cell has three gates, namely, input, forget,  
533 and output gates. These gates can be seen as write (deciding what new information should be kept  
534 in memory by the input gate), reset (deciding what information should be forgotten by the forget  
535 gate), and read (deciding what information should be output by the output gate) operations for the  
536 cells. LSTM cell state is the key component that carries the information between each LSTM cell.  
537 Modifications to the cell state are controlled by the three gates mentioned above. The first stage of  
538 the LSTM cell architecture is the forget gate, which is responsible for specifying which data to  
539 remember and which data to erase. This decision is made through the sigmoid layer as shown in  
540 Equation 2.

541 
$$f_t = \sigma(x_t W^f + h_{t-1} U^f + b_f) \quad (2)$$

542 The output is 0 or 1, where 0 means forget, and 1 means keep. The second stage is the input gate,  
543 which decides which information to be stored or added to the cell state. The input gate also consists  
544 of another sigmoid layer that is used to determine new candidate values that could be updated to  
545 the cell state, as shown in Equation 3.

546 
$$i_t = \sigma(x_t W^i + h_{t-1} U^i + b_i) \quad (3)$$



547 The next stage in LSTM is the memory update, where the old cell is updated to the new cell. The  
 548 *tanh* function creates a vector of candidate values that could be added to the state as shown in  
 549 Equation 4.

$$550 \hat{C}_t = \tanh(x_t W^g + h_{t-1} U^g + b_c) \quad (4)$$

551 The cell state is then ready for the update by concatenating both  $f_t$  and  $\hat{C}_t$ . LSTM updates the old  
 552 cell state  $C_{t-1}$  to be  $C_t$  as shown in Equation 5.

$$553 C_t = \sigma(f_t \times C_{t-1} + i_t \times \hat{C}_t) \quad (5)$$

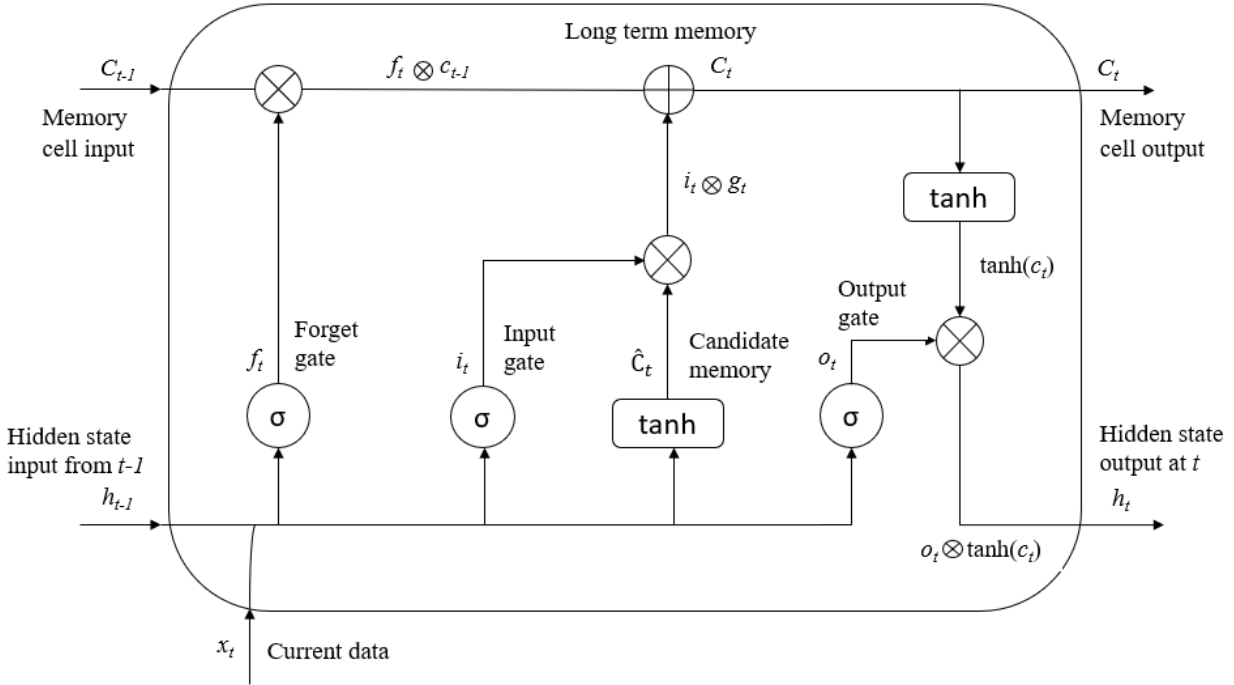
554 The final stage of LSTM is the *output gate*, which uses a sigmoid function to determine which part  
 555 of the cell state will come out as shown in Equation 6.

$$556 o_t = \sigma(x_t W^o + h_{t-1} U^o + b_o) \quad (6)$$

557 In Equation 7, by multiplying  $o_t$  with  $\tanh(C_t)$ , we implicitly determine which part to take out.

$$558 h_t = \tanh(C_t) \times o_t \quad (7)$$

559 Where,  $i_t$ ,  $f_t$ , and  $o_t$  are the input, forget, and output gates, respectively.  $W^i$ ,  $W^f$ , and  $W^o$  are the  
 560 weights for the input, forget, and output gates at time step  $t$ , respectively.  $W^g$  is the weight for the  
 561 candidate layer.  $U^i$ ,  $U^f$ , and  $U^o$  are the weights for the input, forget, and output gates at time step  
 562  $t-1$ .  $U^g$  is the weight for the candidate layer.  $x_t$  is the input at current time step  $t$ .  $h_t$  and  $h_{t-1}$  are the  
 563 output of the cell at current time step  $t$  and previous time step  $t-1$ , respectively.  $C_t$  and  $C_{t-1}$  are the  
 564 cell states at time steps  $t$  and  $t-1$ , respectively.  $b_i$ ,  $b_f$ , and  $b_o$  are the biases for the input, forget, and  
 565 output gates, respectively.  $b_c$  is the bias for the candidate layer, and  $\sigma$  is the sigmoid function.



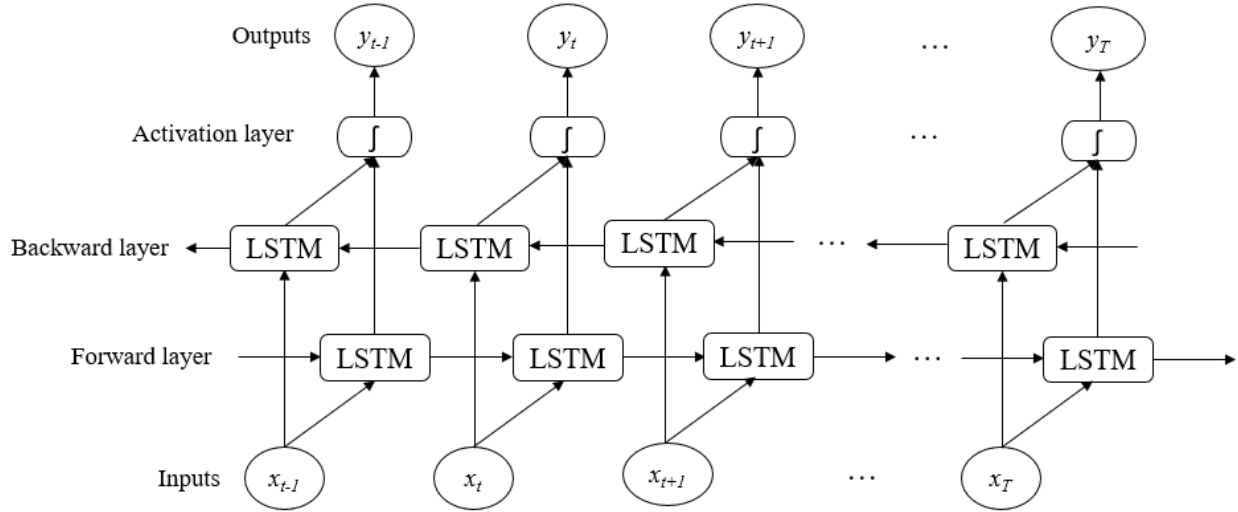
566  
567 **Fig. 5.** LSTM cell architecture

568

569 *4.3.1.2. Bidirectional LSTM (Bi-LSTM)*

570 Fig. 6 depicts the Bi-LSTM layer structure, where the two independent layers share the same input  
 571 sequence while the outputs from the two layers are concatenated and represented in the sequence.  
 572 Bi-LSTM model consists of two separate layers that divide the state neurons of a regular LSTM  
 573 into a forward layer, which is responsible for positive time direction, and a backward layer, which  
 574 is responsible for negative time direction. The outputs of the forward and backward layers are  
 575 concatenated, which make it possible to obtain the forward and backward information at each time  
 576 step in the sequence. This approach enhances the learning process due to the dependency found  
 577 between the neighboring data pairs.

578



579  
580 **Fig. 6.** Bi-LSTM layer structure

581

#### 582 4.3.1.3. Gated recurrent units (GRU)

583 GRU is an improved version of the standard RNN and a simplified version of LSTM (Gers et al.  
584 2002). Like LSTM, GRU is designed to reset or update its memory adaptively. Hence, GRU has a  
585 reset gate and an update gate, which are identical to the forget and the input gates in LSTM. Fig.  
586 7 represents the GRU cell architecture, which is like the LSTM structure but with fewer parameters  
587 that enable it to capture long-term dependencies more easily. The update gate monitors the amount  
588 of memory content that must be forgotten from the previous time step.

589 The operation of a GRU cell can be described as follows:

$$590 z_t = \sigma(W_z \cdot [h_{t-1}, x_t] + b_z) \quad (8)$$

591 The model uses the reset gate to decide the amount of past information to forget as given in  
592 Equation 9.

$$593 r_t = \sigma(W_r \cdot [h_{t-1}, x_t] + b_r) \quad (9)$$

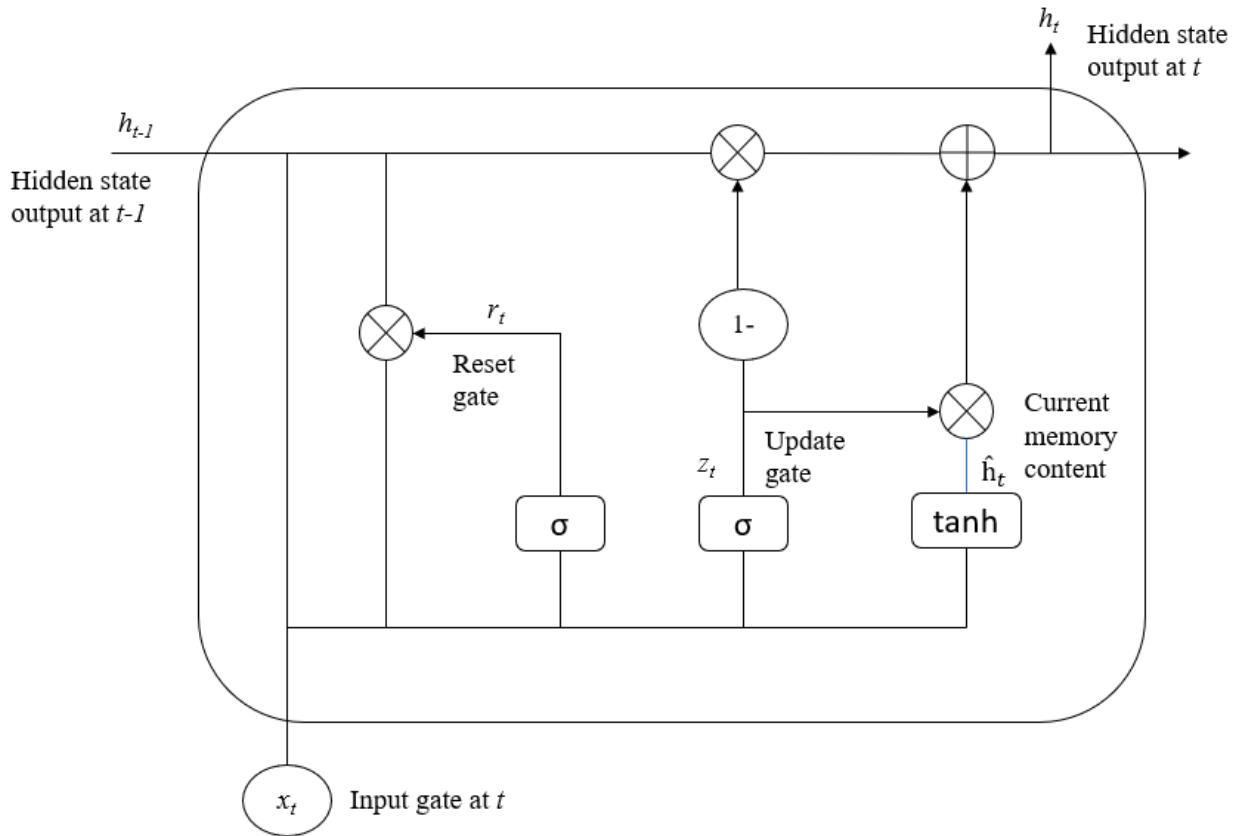
594 New memory content is introduced by using the reset gate as calculated in Equation 9 and relevant  
595 past information is stored as shown in Equation 10.

596  $\hat{h}_t = \tanh(W \cdot [r_t \times h_{t-1}, x_t] + b_h)$  (10)

597 Finally, the network calculates the hidden state  $h_t$ , which is a vector that carries information for  
 598 the current unit and passes it down to the network. Thus, the update gate is essential since it decides  
 599 what is needed from the current memory content  $\hat{h}_t$  and the previous step  $h_{t-1}$ . Equation 11  
 600 calculates the value of  $h_t$ .

601  $h_t = (1 - z_t) \times h_{t-1} + z_t \times \hat{h}_t$  (11)

602 Where,  $z_t$  and  $r_t$  are the output of the update and reset gates.  $W_z$  and  $W_r$  are the weights for the  
 603 update and reset gates.  $b_z$  and  $b_r$  are the biases for the update and reset gates.  $h_t$  and  $h_{t-1}$  are the  
 604 output of the cell at the current time step  $t$  and previous time step  $t-1$ , respectively.  $x_t$  is the input  
 605 at the current time step  $t$ , and  $\sigma$  is the sigmoid function.



606  
 607 **Fig. 7.** GRU cell architecture

#### 608 4.4. *Deep learning model training and performance evaluation*

609 During the deep learning model training, all RNN-based deep learning models (i.e., LSTM, Bi-  
610 LSTM, and GRU) have been designed to receive the same input data. Each class label belongs to  
611 the same participant from plantar pressure data. For each experimental task, the plantar pressure  
612 data vector has a dimensionality of 32 vectors ( $2 \times 16$  pressure sensors for each foot)  $\times$  256 data  
613 samples. The total number of data samples is 4,394 values. Since each window size contains 256  
614 data samples, the current study used input data of 1,124,864 data samples. The network models  
615 are three layers deep, and the number of hidden units ranges from 100 to 500 for each deep learning  
616 model. A previous study used a similar architecture, with 200 hidden units per layer (Alawneh et  
617 al., 2021). In this study, we used the cross-entropy loss (log loss function) as a cost function for  
618 model accuracy. The loss function determines the model's accuracy in the classification problem.  
619 The smaller the loss value, the more accurate the actual value. Updating the weights and biases in  
620 the model is the responsibility of the optimization function. In addition to the Adam optimization  
621 function, an adaptive version of the stochastic gradient descent was used for model training  
622 (Kingma and Ba, 2014). The Adam optimizer is a reliable optimizer that ensures fast and accurate  
623 results when updating the network parameters. To prevent overfitting in the model, this study  
624 applied the widely used stochastic regularization method known as the dropout technique  
625 (Srivastava et al., 2014). Overfitting arises when the loss function is very small for training data  
626 while it is very large for testing data. The main objective of the dropout technique is to prevent the  
627 neurons in the network from excessive co-adapting, which results in a lack of model generalization.  
628 The model evaluation process is performed by dividing the dataset into training and testing datasets,  
629 thus, 90% for training and the remaining 10% for testing. The training dataset was further split  
630 into two datasets (80% for training and 20% for validation). The validation dataset was used for

631 hyper-parameter tuning and to determine the optimal unit numbers of the RNN-based deep  
632 learning models. The 10-folds cross-validation technique was adopted to test the classification  
633 performance of RNN-based deep learning models, similar to previous studies utilizing deep  
634 learning networks (Kim and Cho, 2020; Yang et al., 2020). By conducting 10-folds cross-  
635 validation, the best hyper-parameters can be selected, and the RNN-based deep learning models  
636 can be evaluated as generalized models that show the desired classification performance with an  
637 unseen dataset. The parameters values based on the model that provided the best accuracy with the  
638 lowest training time were selected. The results show that our tuning process achieved the best  
639 accuracy for the datasets when setting the values of the epoch, dropout, batch size, learning rate,  
640 and hidden units at 100, 0.5, 64, 0.001, and 200, respectively. The experiments were conducted  
641 and trained on a computer 2.60 GHz Intel (R) Core (TM) i7-9750H CPU, 16GB RAM, 64-bit  
642 operating system, Windows 10 Pro, and Intel Iris Plus Graphics 650 1536MB GPU using  
643 MATLAB R2020b. The detailed dataset and tuned hyper-parameters of the proposed RNN-based  
644 deep learning models are shown in Table 1.

645 **Table 1.** Dataset and hyper-parameters of the proposed RNN-based deep learning models

<b>Dataset and hyper-parameters</b>	<b>Value</b>
Number of classes	5
Number of plantar pressure sensors	32 capacitive pressure sensors
Window size	5.12 s
Overlap of adjacent windows	50%
Sampling rate	50 Hz
Epoch	100
Dropout	0.5
Batch size	64
Learning rate	0.001
Hidden units	200
Number of sample data	1,125,000 data samples

646  
647 In performance evaluation and classification, the performance of the three types of RNN-based  
648 deep learning models was assessed by using evaluation metrics such as accuracy, precision, recall,

649 specificity, and F1-score (Attal et al. 2015). Equations 12 to 16 show how each evaluation metric  
650 is calculated. Accuracy is the most standard metric to summarize the overall classification  
651 performance for all classes. It is defined as the ratio of correctly classified instances to the total  
652 number of instances. Precision is the measure of determining how many instances classified as  
653 positive are actually positive, thus, it is a measure of exactness. It is defined as the ratio of correctly  
654 classified positive instances to the total number of instances classified as positive. Recall or  
655 sensitivity is the number of positive instances correctly classified as positive, thus, it is a measure  
656 of correctness. It is defined as the ratio of correctly classified positive instances to the total number  
657 of positive instances. Specificity is the number of negative instances correctly classified as  
658 negative. It is defined as the ratio of correctly classified negative instances to the total number of  
659 instances classified as negative. The F1-score combines precision and recall into a single value,  
660 and it is used to measure the performance of the classification model by avoiding systematic bias  
661 (Ordóñez and Roggen, 2016). Besides these evaluation metrics, the performance of each model on  
662 individual classes was assessed using a confusion matrix, while the accuracy and loss curves were  
663 drawn for the best model.

$$664 \text{ Accuracy} = \frac{TP + TN}{TP + TN + FP + FN} \quad (12)$$

$$665 \text{ Precision} = \frac{TP}{TP + FP} \quad (13)$$

$$666 \text{ Recall} = \frac{TP}{TP + FN} \quad (14)$$

$$667 \text{ Specificity} = \frac{TN}{TN + FP} \quad (15)$$

$$668 \text{ F1 - score} = 2 \times \frac{\text{Precision} \times \text{Recall}}{\text{Precision} + \text{Recall}} \quad (16)$$

669 Where, True Positive (TP) is the number of positive instances that were classified as positive, True  
670 Negative (TN) is the number of negative instances that were classified as negative, False Positive  
671 (FP) is the number of negative instances that were classified as positive, and False Negatives (FN)  
672 is the number of positive instances that were classified as negative.

673

## 674 5. Results

675 This section presents the results derived from the conducted experimental design and data  
676 collection procedures. Table 2 shows the classification accuracy and training time for different  
677 types of RNN-based deep learning models which were evaluated by 10-folds cross-validation. The  
678 classification accuracy for all three RNN-based deep learning models was greater than 97%. As  
679 indicated in Table 2, the classification accuracies were 97.99%, 98.33%, and 99.01% for LSTM,  
680 Bi-LSTM, and GRU, respectively. The results revealed that GRU model achieved the highest  
681 performance among all tested RNN-based deep learning models in terms of training plantar  
682 pressure pattern data for classifying different types of awkward working postures. On the other  
683 hand, when the performance of the three types of RNN-based deep learning models was evaluated  
684 in terms of training time, the average duration of LSTM, Bi-LSTM, and GRU networks lasted 31  
685 mins, 56 mins, and 54 mins, respectively. The results show that Bi-LSTM network requires more  
686 training time than either LSTM or GRU models.

687 **Table 2.** Classification accuracy and training time for RNN-based deep learning models

<b>RNN-based deep learning models</b>	<b>Accuracy (%)</b>	<b>Training time (minutes)</b>
Long-short term memory (LSTM)	97.99	31
Bidirectional LSTM (Bi-LSTM)	98.33	56
Gated recurrent units (GRU)	99.01	54

688

689 The confusion matrix and evaluation metrics for LSTM model are presented in Table 3. Generally,  
690 the evaluation metrics achieved high performance of LSTM model on the plantar pressure data for



691 classifying different types of awkward working postures. In terms of precision metric, LSTM  
692 model achieved classification performance values between 88.30% and 99.82%. The highest  
693 instance of correct classified awkward working posture was overhead working posture,  
694 representing 98.74%. Conversely, stooping posture had little impact on the LSTM model (i.e.,  
695 67.48%) among the different types of awkward working postures. The values of specificity and  
696 F1-score metrics are in the range of 95.33% to 99.94%, and 76.50% to 98.40%, respectively. To  
697 identify the classes that are misclassified or confused with other classes, the confusion matrix was  
698 presented. As shown in Table 3, each row represents the actual classes, while the columns represent  
699 the predicted classes. The diagonal cells represent the correct instances as highlighted in bold font  
700 for a more detailed evaluation of the classification performance at the end of the 100<sup>th</sup> epoch. The  
701 other cells show the misclassified instances. From Table 3, it was revealed that overhead working  
702 posture class had the best recognition performance because plantar pressure data are different from  
703 the values in other classes. It can also be seen that the top two most misclassified classes are  
704 stooping and overhead working postures. Stooping posture is confused 30 times with overhead  
705 working posture. Data collection for both stooping and overhead working postures involved  
706 bilateral knee extension in static positions. As such, the confusion between stooping and overhead  
707 working postures can be explained by the similar plantar pressure data collected from the wearable  
708 insole system.

709 **Table 3.** Confusion matrix and evaluation metrics for long-short term memory (LSTM)

		Predicted class				
		Overhead working	Squatting	Stooping	Semi-squatting	One-legged kneeling
True class	Overhead working	<b>625</b>	0	5	3	0
	Squatting	10	<b>350</b>	4	3	1
	Stooping	30	4	<b>83</b>	6	0
	Semi-squatting	23	0	2	<b>433</b>	0
	One-legged kneeling	8	0	0	9	<b>533</b>
		Overhead working	Squatting	Stooping	Semi-squatting	One-legged kneeling
<b>Accuracy</b>						97.99%
<b>Precision</b>		89.80%	98.87%	88.30%	95.37%	99.82%
<b>Recall</b>		98.74%	95.11%	67.48%	94.54%	97.02%
<b>Specificity</b>		95.33%	99.78%	99.46%	98.76%	99.94%
<b>F1-score</b>		94.06%	96.95%	76.50%	94.96%	98.40%

710

711 Table 4 represents the confusion matrix and evaluation metrics of Bi-LSTM model. The correct  
712 classes are shown in bold for a more detailed evaluation of the classification performance at the  
713 end of the 100<sup>th</sup> epoch. Generally, the evaluation metrics of Bi-LSTM model achieved higher  
714 performance than LSTM model. With regards to precision metric, Bi-LSTM model achieved  
715 performance rates between 92.09% and 99.61%. Like LSTM model, the highest instance of Bi-  
716 LSTM for correct classified awkward working posture was overhead working, representing  
717 97.83%. It was reported that overhead working posture had the most positive impact on the  
718 performance of Bi-LSTM, followed by one-legged kneeling (97.80%), squatting (96.37%), semi-  
719 squatting (93.02%), and stooping (87.50%) (Table 4). The specificity and F1-score metrics of  
720 different types of awkward working postures range from 96.03% to 99.88% and 91.70% to 98.75%,  
721 respectively. According to the confusion matrix in Table 4, it can be observed that overhead  
722 working posture is the most recognized class with 675 positive instances. In addition, it was found  
723 that the top two most misclassified classes are stooping and overhead working postures (Table 4).

724

725 **Table 4.** Confusion matrix and evaluation metrics for bidirectional LSTM (Bi-LSTM)

		Predicted class				
		Overhead working	Squatting	Stooping	Semi-squatting	One-legged kneeling
True class	Overhead working	<b>675</b>	0	8	5	2
	Squatting	8	<b>425</b>	0	8	0
	Stooping	25	2	<b>210</b>	3	0
	Semi-squatting	18	0	0	<b>240</b>	0
	One-legged kneeling	7	0	0	4	<b>512</b>
		Overhead working	Squatting	Stooping	Semi-squatting	One-legged kneeling
<b>Accuracy</b>						98.33%
<b>Precision</b>		92.09%	99.53%	96.33%	92.31%	99.61%
<b>Recall</b>		97.83%	96.37%	87.50%	93.02%	97.80%
<b>Specificity</b>		96.03%	99.88%	99.58%	98.94%	99.88%
<b>F1-score</b>		94.87%	97.93%	91.70%	92.66%	98.75%

726

727 The confusion matrix and evaluation metrics of GRU model are presented in Table 5 with correct

728 classes shown in bold for a more detailed evaluation of the classification performance at the end

729 of the 100<sup>th</sup> epoch. The evaluation metrics of GRU model achieved the highest performance

730 compared to either LSTM or Bi-LSTM model. Regarding precision metric, GRU model achieved

731 classification performance values between 94.41% and 99.80%. The highest instance of correct

732 classified awkward working posture was overhead working, representing 99.30%. This recall

733 result concurs with classification accuracy, thus, indicating that GRU model outperforms other

734 RNN-based deep learning models. It was found that stooping posture had the lowest correct

735 classified posture (i.e., 89.00%) among the different types of awkward working postures. The

736 specificity and F1-score metrics of different types of awkward working postures range from 97.08%

737 to 99.94% and 93.19% to 99.39%, respectively. Taken together, these results show that GRU

738 model outperformed either LSTM or Bi-LSTM model based on plantar pressure data for

739 classifying different types of awkward working postures. Like LSTM and Bi-LSTM models, it can

740 be observed from the confusion matrix in Table 5 that overhead working posture is the most

741 recognized class with 710 positive instances. Moreover, it was reported that stooping and overhead  
 742 working postures are the top two most misclassified classes (Table 5).

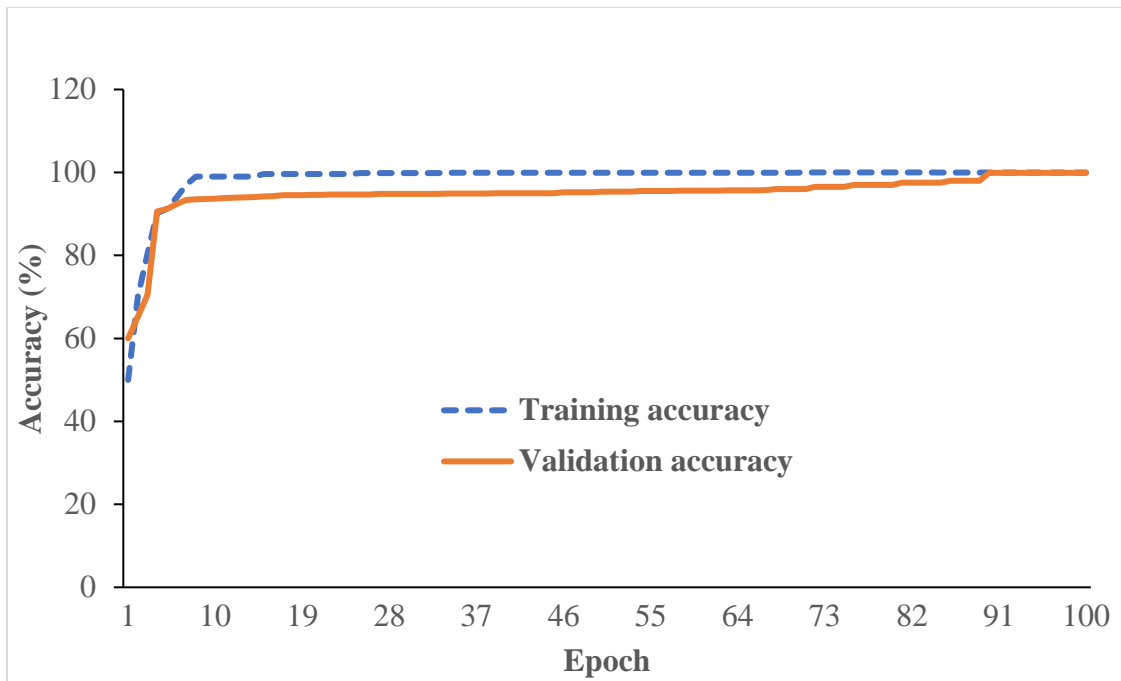
743

744 **Table 5.** Confusion matrix and evaluation metrics for gated recurrent units (GRU)

		<b>Predicted class</b>				
<b>True class</b>	Overhead working	<b>710</b>	0	4	1	0
	Squatting	5	<b>412</b>	0	3	0
	Stooping	21	1	<b>178</b>	0	0
	Semi-squatting	12	0	0	<b>310</b>	1
	One-legged kneeling	4	0	0	1	<b>489</b>
		Overhead working	Squatting	Stooping	Semi-squatting	One-legged kneeling
<b>Accuracy</b>						99.01%
<b>Precision</b>		94.41%	99.76%	97.80%	98.41%	99.80%
<b>Recall</b>		99.30%	98.10%	89.00%	95.98%	98.99%
<b>Specificity</b>		97.08%	99.94%	99.80%	99.73%	99.94%
<b>F1-score</b>		96.80%	98.92%	93.19%	97.18%	99.39%

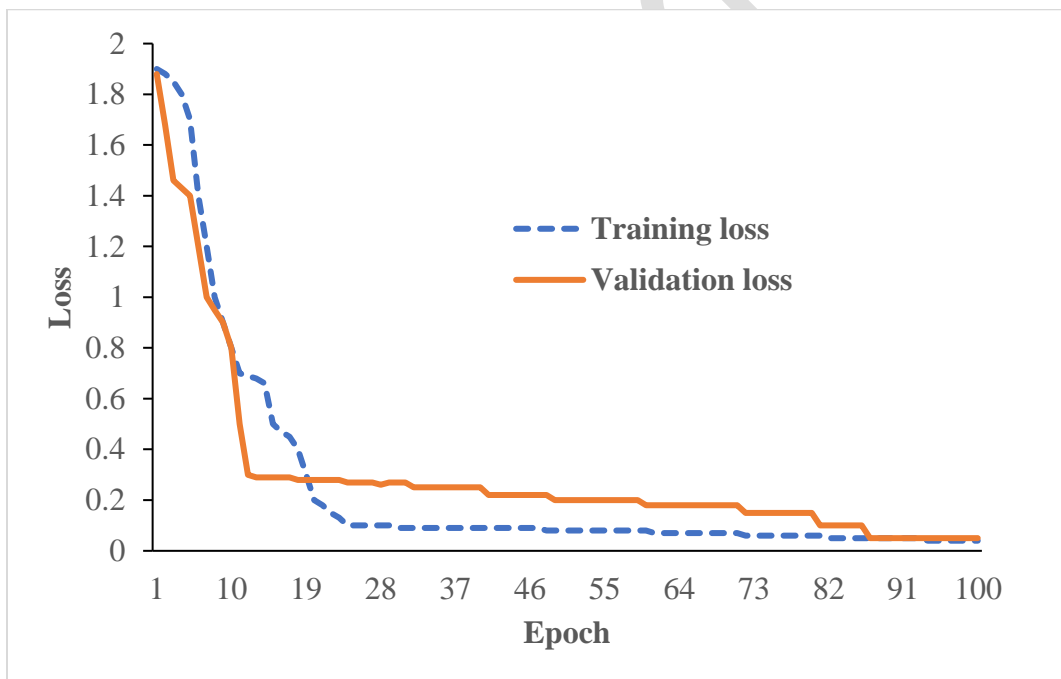
745

746 Fig. 8 and 9 show the accuracies and losses over iterations curves with the tuned hyperparameters  
 747 of the GRU model. As shown in both figures, GRU model performance shows an increase in  
 748 accuracy and decrease in loss in both training and validation, respectively. In other words, the  
 749 training and validation curves for GRU model converge at higher accuracy whilst their  
 750 corresponding loss curves converge at a lower loss value. It was found that both the accuracies and  
 751 losses were converged at the 90<sup>th</sup> epoch. Thus, the difference between either training accuracy and  
 752 validation accuracy or training loss and validation loss was insignificant, indicating that the GRU  
 753 model was effectively trained without overfitting plantar pressure data.



754  
755  
756

**Fig. 8.** Accuracies over iterations curves with the tuned hyperparameters of the GRU model



757  
758  
759

**Fig. 9.** Losses over iterations curves with the tuned hyperparameters of the GRU model

760 6. **Discussion**

761 *6.1. Wearable sensing data and deep learning-based networks*

762 Construction activities are associated with several work-related risk factors. Among them,  
763 awkward working postures are the major risk factor that causes WMSDs in construction. The  
764 objective of this research was to evaluate a novel approach of using deep learning-based networks  
765 and wearable insole sensor data to automatically recognize and classify different types of awkward  
766 working postures in construction. To do this, this study adopted three types of RNN-based deep  
767 learning models to train time-series plantar pressure data captured by a wearable insole system.

768  
769 By comparing the employed RNN-based deep learning models in this study, it was found that  
770 GRU model achieved the highest accuracy (i.e., 99.01%) with an average training duration of 54  
771 minutes. In addition, the results show that GRU model obtained precision, recall, specificity, and  
772 F1-score metrics of 94.41% to 99.80%, 89.00% to 99.30%, 97.08% to 99.94%, and 93.19% to  
773 99.39%, respectively in classifying different types of awkward working postures. Regarding the  
774 confusion matrix, it was revealed that the top two most misclassified classes are stooping and  
775 overhead working postures. Moreover, GRU model performance shows an increase in accuracy  
776 and a decrease in loss in both training and validation, respectively. These results support the  
777 hypothesis of this study that GRU model, which is an RNN-based deep learning network could  
778 provide a reliable and better performance accuracy for classifying different types of awkward  
779 working postures. This finding might be explained from the model perspective. GRU model is  
780 relatively simpler and can forget and choose memory with fewer parameters, while LSTM model  
781 needs more gating and parameters to complete similar tasks. In addition, GRU model can control  
782 the information flow from the previous activation when computing new candidate activation. In

783 summary, GRU model outperformed other RNN-based deep learning models in this study in terms  
784 of computational power (i.e., convergence of training time) and performance (i.e., parameter  
785 updates). Our results are comparable to other previous studies which found GRU model to  
786 outperform LSTM model (Yang et al., 2020; Zarzycki and Ławryńczuk, 2021). The findings of  
787 this study indicate that GRU architecture can leverage the advantages of both LSTM and Bi-LSTM  
788 layer architectures to enhance awkward posture recognition. Hence, the use of the GRU model is  
789 recommended for classifying awkward working postures based on wearable insole data.

790

791 A previous study by Antwi-Afari et al. (2018f) utilized plantar pressure data to recognize different  
792 types of awkward working postures based on machine learning classifiers, finding an accuracy of  
793 99.70% with SVM classifier at 0.32s window size. However, this previous work was conducted in  
794 a controlled laboratory setting, by student participants, and static awkward working postures.  
795 These experimental conditions are not the case in a real-world construction environment. By  
796 utilizing WIMU-based systems, Lee et al. (2020) compared a deep learning network (i.e., CNN-  
797 LSTM) to conventional machine learning classifiers for automated classification of squat postures.  
798 They obtained 75.4% and 91.7% classification performance for conventional machine learning  
799 and deep learning model, respectively. Although these results are comparable to the current study,  
800 Lee et al. (2020) used acceleration and angular velocity data while the present study used plantar  
801 pressure data captured by a wearable insole system.

802

803 Notably, previous studies have also demonstrated similar deep learning networks (e.g., vanilla,  
804 unidirectional LSTM, Bi-LSTM, GRU) in wearable sensor-based human activity recognition  
805 studies in construction (Rashid and Louis, 2019; Kim and Cho, 2020; Lee et al., 2020; Yang et al.,

2020; Zhao and Obonyo, 2021) and other disciplines (Li et al., 2019; Alawneh et al., 2021; Mekuksavanich and Jitpattanakul, 2021). Rashid and Louis (2019) evaluated a data-augmentation framework for identifying construction equipment activity by combining LSTM model and multiple WIMU-based systems. They found that LSTM model outperforms conventional machine learning classifier (i.e., artificial neural network). Kim and Cho (2020) proposed a construction worker's motion recognition model using the LSTM network based on an evaluation of the number and location of WIMUs to maximize motion recognition performance. They found that the proposed approach could improve a worker monitoring mechanism for safety and productive management. Yang et al. (2020) investigated the feasibility of identifying various physical loading conditions by analyzing a worker's bodily movements collected by using WIMUs. Their findings contribute to automated work-related risk recognition and WMSDs prevention, thus, enhancing workers' health and safety at construction workplace. Zhao and Obonyo (2020) investigated the feasibility of integrating convolutional neural networks (CNN) with LSTM layers for recognizing construction workers' postures from motion captured by WIMUs-based systems. The results revealed that the proposed deep neural network approach has a high potential in addressing challenges for improving posture recognition performance than conventional machine learning models. Alawneh et al. (2021) compared the performance of data augmentation and RNN-based deep learning models on three open-source datasets, finding that GRU models and data augmentation significantly enhance activity recognition. Collectively, these studies found that deep learning models and wearable sensing data can be utilized for monitoring workers' activities regarding their safety, fall risks, and productivity. However, direct comparison between existing studies' findings and the current study may not be meaningful due to numerous differences in experimental design (e.g., participants' physical characteristics) and data collection procedures.



829 *6.2. Study implications, practical applications, and contributions*

830 The current study provides relevant findings and practical implications to both researchers and  
831 practitioners within the construction industry. First, a key practical implication is the feasibility of  
832 onsite experimental data collection for work-related risk factor recognition using a wearable insole  
833 pressure system. Collecting wearable sensing data in a real-world construction setting is very  
834 challenging due to multiple reasons such as the dynamic nature of the construction environment,  
835 huge resources, and several work-related risk factors. Different from previous studies on work-  
836 related risk factor recognition that were conducted by student participants in a controlled  
837 laboratory setting (Chen et al., 2017; Antwi-Afari et al., 2018f; Umer et al., 2020), the current  
838 study investigated the use of wearable insole data while construction rebar workers performed  
839 awkward working postures during repetitive rebar tasks at construction site. Awkward working  
840 postures are also commonly performed by other workers such as masons, carpenters in the  
841 construction industry. Collectively, the proposed approach could not only be applied during  
842 repetitive rebar tasks (e.g., preparing and assembling rebars), but also other manual repetitive  
843 handling tasks (e.g., bricklaying) in construction. Second, the proposed approach provides an  
844 automated recognition and classification of awkward working postures in construction. The results  
845 from the current study revealed that awkward working postures, the most prevalent work-related  
846 risk factor among construction workers, could be recognized and classified by using wearable  
847 insole data and deep learning networks. Awkward posture recognition is the first step in proactive  
848 WMSD prevention. As such, this wearable sensor-based approach can serve as a proactive  
849 intervention tool for recognizing work-related risk factors, thus, mitigating WMSDs risks in  
850 construction. Besides automated WMSDs risk monitoring and recognition in construction, the  
851 achieved awkward posture recognition model can also facilitate “Prevention through Design” (PtD)

852 practices by identifying workers' ergonomic risks under different workplace designs. These  
853 preventive strategies can also be adopted in other physically demanding and labor-intensive  
854 occupations such as manufacturing, automobile, and agriculture. Third, the proposed approach—  
855 utilizing wearable insole data and deep learning-based networks—will contribute to real-time  
856 wearable sensor computing by deploying the performance of plantar pressure patterns and GRU  
857 model for awkward posture recognition. Construction practitioners (e.g., safety managers) can use  
858 this piece of information to enhance their safety program, thus, improving workers' safety and  
859 health. With the performance accuracies of three RNN-based deep learning models in this study,  
860 the best RNN-based deep learning model (i.e., GRU) can learn workers' movement patterns and  
861 provide reliable results for predicting posture-based WMSDs risk. However, it was found that  
862 stooping and overhead working postures were misclassified and could lead to recognition errors.  
863 Nevertheless, the findings of this study can be applied to other work-related risk factors (e.g.,  
864 overexertion, loss of balance events) with specific physical load conditions and reasonable hyper-  
865 parameter tuning through model training and testing, thus, mitigating the risk of developing  
866 WMSDs.

867

### 868 *6.3. Limitations and future research directions*

869 The proposed approach is successful for automated recognition and classification of awkward  
870 working postures in construction. However, there are few limitations and challenges. First, this  
871 study only investigated a small sample of experienced rebar workers and five types of awkward  
872 working postures in construction. With diverse construction workers and physically demanding  
873 construction activities, the small experimental dataset could limit the application of the proposed  
874 approach in the construction industry. Future studies should collect large samples of data from

875 several construction workers (e.g., bricklayers, carpenters) while conducting other types of  
876 awkward working postures (e.g., bending or twisting to lift an object) during a real-world  
877 construction environment. Such dataset with enough samples is crucial in training, testing, and  
878 developing a generalized model for different construction activities. Second, this study considered  
879 limited types of wearable sensor data—plantar pressure data—for automated recognition of  
880 awkward working posture. Notably, there are other types of body sensor networks or wearable  
881 biosensors for collecting heart rate, respiration, and body temperature data could be integrated to  
882 enhance automated monitoring and recognition applications. As such, future research should  
883 include other types of biosensor data. Third, the current study employed only three types of RNN-  
884 based deep learning models for awkward posture recognition and classification. Although useful,  
885 RNN-based deep learning models are specifically designed to handle sequential data, but they  
886 suffer from the vanishing/exploding gradient problem. As a result, RNNs fail to deal with long  
887 sequences if *tanh* is applied as the activation function, whereas the model is unstable if a rectified  
888 linear unit (*relu*) is used (Dang et al., 2020). In addition, RNN layers cannot be stacked into a very  
889 deep model because the saturated activation functions cause the gradient to decay over layers.  
890 Consequently, future research could evaluate other types of deep learning networks (e.g., CNN)  
891 or integrate two or more deep learning networks (e.g., CNN-LSTM) for awkward posture  
892 recognition.

893

## 894 **7. Conclusions**

895 This research evaluates a novel approach of using deep learning-based networks and wearable  
896 insole sensor data to automatically recognize and classify different types of awkward working  
897 postures in construction, which may lead workers to develop WMSDs. Five different types of

898 awkward working postures (i.e., overhead working, squatting, stooping, semi-squatting, and one-  
899 legged kneeling) were conducted, and plantar pressure data were captured by using a wearable  
900 insole pressure system. The classification performance of three RNN-based deep learning  
901 models—LSTM, Bi-LSTM, and GRU— was evaluated using metrics such as accuracy, precision,  
902 recall, specificity, and F1-score. The experimental results show that GRU model outperforms the  
903 other RNN-based deep learning models with a high accuracy of 99.01% and F1-score between  
904 93.19% and 99.39%. These results suggest that GRU model, widely applied for the classification  
905 of time-series and sequential data, can be employed to learn sequential plantar pressure patterns  
906 captured by a wearable insole system to recognize and classify different types of awkward working  
907 postures. The proposed approach will contribute to real-time wearable insole sensor computing by  
908 deploying the performance of GRU model for awkward working posture recognition on  
909 construction sites. In addition, it contributes to automated WMSDs risk recognition among  
910 construction workers by enabling safety managers to continuously monitor awkward working  
911 postures, thus improving workers' safety and health conditions. To develop a detailed practical  
912 guideline for this application, future research could integrate other types of wearable biosensors  
913 (e.g., heart rate monitors) and deep learning networks (e.g., CNN) for vigorous recognition of  
914 awkward working postures.

915

#### 916 **Data availability statement**

917 The datasets used in this study are available from the corresponding author upon request.

918

#### 919 **Declaration of competing interest**

920 None

921 **Acknowledgement**

922 The authors acknowledged supports from (1) Aston Institute for Urban Technology and the  
923 Environment (ASTUTE), Seedcorn Grants Proposal 2020/21 entitled “Wearable Insole Sensor  
924 Data and a Deep Learning Network-Based Recognition for Musculoskeletal Disorders Prevention  
925 in Construction” and (2) Aston Research and Knowledge Exchange Pump Priming Fund 2021/22  
926 on a Grant Proposal entitled “Digital Twin-Enabled Wearable Sensing Technologies for Improved  
927 Workers’ Activity Recognition and Work-Related Risk Assessment”. Special thanks to all our  
928 participants involved in this study.

929

930 **References**

- 931 Akhavian, R., and Behzadan, A. H. (2016) Smartphone-based construction workers' activity  
932 recognition and classification. *Automation in Construction*, Vol. 71, No. 2, pp. 198–209.  
933 DOI: <https://doi.org/10.1016/j.autcon.2016.08.015>.
- 934 Alawneh, L., Alsarhan, T., Al-Zinati, M., Al-Ayyoub, M., Jararweh, Y., and Lu, H. (2021)  
935 Enhancing human activity recognition using deep learning and time series augmented  
936 data. *Journal of Ambient Intelligence and Humanized Computing*, pp. 1-16. DOI:  
937 <https://doi.org/10.1007/s12652-020-02865-4>.
- 938 Alwasel, A., Abdel-Rahman, E. M., Haas, C. T., and Lee, S. (2017) Experience, productivity, and  
939 musculoskeletal injury among masonry workers. *Journal of Construction Engineering and  
940 Management*, Vol. 143, No. 6, pp. 05017003. DOI:  
941 [https://doi.org/10.1061/\(ASCE\)CO.1943-7862.0001308](https://doi.org/10.1061/(ASCE)CO.1943-7862.0001308).
- 942 Antwi-Afari, M. F., and Li, H. (2018g) Fall risk assessment of construction workers based on  
943 biomechanical gait stability parameters using wearable insole pressure system. *Advanced  
944 Engineering Informatics*, Vol. 38, pp. 683-694. DOI:  
945 <https://doi.org/10.1016/j.aei.2018.10.002>.
- 946 Antwi-Afari, M. F., Li, H., Edwards, D. J., Pärn, E. A., Owusu-Manu, D., Seo, J., and Wong, A.  
947 Y. L. (2018a) Identification of potential biomechanical risk factors for low back disorders  
948 during repetitive rebar lifting. *Construction Innovation*, Vol. 18, No. 2. DOI:  
949 <https://doi.org/10.1108/CI-05-2017-0048>.
- 950 Antwi-Afari, M. F., Li, H., Seo, J., and Wong, A. Y. L. (2018e) Automated detection and  
951 classification of construction workers’ loss of balance events using wearable insole  
952 pressure sensors. *Automation in Construction*, Vol. 96, pp. 189-199. DOI:  
953 <https://doi.org/10.1016/j.autcon.2018.09.010>.
- 954 Antwi-Afari, M. F., Li, H., Umer, W., Yu, Y., and Xing, X. (2020a) Construction activity  
955 recognition and ergonomic risk assessment using a wearable insole pressure system.  
956 *Journal of Construction Engineering and Management*, Vol. 146, No. 7, pp. 04020077.  
957 DOI: [https://doi.org/10.1061/\(ASCE\)CO.1943-7862.0001849](https://doi.org/10.1061/(ASCE)CO.1943-7862.0001849).

958 Antwi-Afari, M. F., Li, H., Wong, J. K W., Oladinrin, O., Ge, J. X., Seo, J., and Wong, A. Y. L.  
959 (2019a) Sensing and warning based technology applications to improve occupational  
960 health and safety in the construction industry: A Literature Review. *Engineering,*  
961 *Construction and Architectural Management*, Vol. 26, No. 8, pp. 1534-1552. DOI:  
962 <https://doi.org/10.1108/ECAM-05-2018-0188>.

963 Antwi-Afari, M. F., Li, H., Yu, Y., and Kong, L. (2018f) Wearable insole pressure system for  
964 automated detection and classification of awkward working postures in construction  
965 workers. *Automation in Construction*, Vol. 96, pp. 433-441. DOI:  
966 <https://doi.org/10.1016/j.autcon.2018.10.004>.

967 Anwer, S., Li, H., Antwi-Afari, M. F., and Wong, A. L. Y. (2021) Associations between physical  
968 or psychosocial risk factors and work-related musculoskeletal disorders in construction  
969 workers based on literature in the last 20 years: A systematic review. *International Journal*  
970 *of Industrial Ergonomics*, Vol. 83, pp. 103113. DOI:  
971 <https://doi.org/10.1016/j.ergon.2021.103113>.

972 Anwer, S., Li, H., Antwi-Afari, M. F., Umer, W., Mehmood, I., Al-Hussein, M., and Wong, A. Y.  
973 L. (2021) Test-retest reliability, validity, and responsiveness of a textile-based wearable  
974 sensor for real-time assessment of physical fatigue in construction bar benders. *Journal of*  
975 *Building Engineering*, Vol. 44, pp. 103348. DOI:  
976 <https://doi.org/10.1016/j.jobe.2021.103348>.

977 Attal, F., Mohammed, S., Dedabrishvili, M., Chamroukhi, F., Oukhellou, L., and Amirat, Y. (2015)  
978 Physical human activity recognition using wearable sensors. *Sensors*, Vol. 15, No. 12, pp.  
979 31314-31338. DOI: <https://doi.org/10.3390/s151229858>.

980 Bao, L., and Intille, S. S. (2004) Activity recognition from user-annotated acceleration data.  
981 In *International Conference on Pervasive Computing*, pp. 1-17, Springer, Berlin,  
982 Heidelberg. DOI: [https://doi.org/10.1007/978-3-540-24646-6\\_1](https://doi.org/10.1007/978-3-540-24646-6_1).

983 Buchholz, B., Paquet, V., Wellman, H. and Forde, M. (2003) Quantification of ergonomic hazards  
984 for ironworkers performing concrete reinforcement tasks during heavy highway  
985 construction. *American Industrial Hygiene Association Journal*, Vol. 64, No. 2, pp. 243-  
986 250. DOI: <http://dx.doi.org/10.1080/15428110308984814>.

987 Caldas, C. H., Torrent, D. G., and Haas, C. T. (2006) Using global positioning system to improve  
988 materials-locating processes on industrial projects. *Journal of Construction Engineering*  
989 *and Management*, Vol. 132, No. 7, pp. 741-749. DOI:  
990 [https://doi.org/10.1061/\(ASCE\)0733-9364\(2006\)132:7\(741\)](https://doi.org/10.1061/(ASCE)0733-9364(2006)132:7(741)).

991 Center for Construction Research and Training (CPWR) (2018) *The Construction Chart*  
992 *Book: The United States Construction Industry and Its Workers*, sixth edition, Silver  
993 Spring, MD 20910. Available at: [https://www.cpwr.com/wp-](https://www.cpwr.com/wp-content/uploads/publications/The_6th_Edition_Construction_eChart_Book.pdf)  
994 [content/uploads/publications/The\\_6th\\_Edition\\_Construction\\_eChart\\_Book.pdf](https://www.cpwr.com/wp-content/uploads/publications/The_6th_Edition_Construction_eChart_Book.pdf) (Accessed:  
995 August 2021).

996 Chen, J., Qiu, J., and Ahn, C. (2017) Construction worker's awkward posture recognition through  
997 supervised motion tensor decomposition. *Automation in Construction*, Vol. 77, pp. 67-81.  
998 DOI: <https://doi.org/10.1016/j.autcon.2017.01.020>.

999 Chen, Y., and Shen, C. (2017) Performance analysis of smartphone-sensor behavior for human  
1000 activity recognition. *IEEE Access*, Vol. 5, pp. 3095-3110. DOI:  
1001 <https://doi.org/10.1109/ACCESS.2017.2676168>.

1002 Dang, L. M., Min, K., Wang, H., Piran, M. J., Lee, C. H., and Moon, H. (2020) Sensor-based and  
1003 vision-based human activity recognition: A comprehensive survey. *Pattern*  
1004 *Recognition*, Vol. 108, pp. 107561. DOI: <https://doi.org/10.1016/j.patcog.2020.107561>.

1005 David, G. C. (2005) Ergonomic methods for assessing exposure to risk factors for work-related  
1006 musculoskeletal disorders. *Occupational Medicine*, Vol. 55, No. 3, pp. 190–199. DOI:  
1007 <https://doi.org/10.1093/occmed/kqi082>.

1008 De Dominicis, C. M., Depari, A., Flammini, A., Rinaldi, S., and Sisinni, E. (2013) Smartphone  
1009 based localization solution for construction site management. In *2013 IEEE Sensors*  
1010 *Applications Symposium Proceedings*, pp. 43-48. DOI:  
1011 <https://doi.org/10.1109/SAS.2013.6493554>.

1012 Delrobaei, M., Memar, S., Pieterman, M., Stratton, T. W., McIsaac, K., and Jog, M. (2018)  
1013 Towards remote monitoring of Parkinson’s disease tremor using wearable motion capture  
1014 systems. *Journal of the Neurological Sciences*, Vol. 384, pp. 38-45. DOI:  
1015 <https://doi.org/10.1016/j.jns.2017.11.004>.

1016 Fang, Q., Li, H., Luo, X., Ding, L., Luo, H., Rose, T. M., and An, W. (2018) Detecting non-  
1017 hardhat-use by a deep learning method from far-field surveillance videos. *Automation in*  
1018 *Construction*, Vol. 85, pp. 1-9. DOI: <https://doi.org/10.1016/j.autcon.2017.09.018>.

1019 Fang, W., Ding, L., Luo, H., and Love, P. E. (2018) Falls from heights: A computer vision-based  
1020 approach for safety harness detection. *Automation in Construction*, Vol. 91, pp. 53-61.  
1021 DOI: <https://doi.org/10.1016/j.autcon.2018.02.018>.

1022 Gers, F. A., Schraudolph, N. N., and Schmidhuber, J. (2002) Learning precise timing with LSTM  
1023 recurrent networks. *Journal of Machine Learning Research*, Vol. 3, No. 1, pp. 115-143.  
1024 Available via:  
1025 [https://search.ebscohost.com/login.aspx?direct=true&db=bth&AN=9793888&site=eds-](https://search.ebscohost.com/login.aspx?direct=true&db=bth&AN=9793888&site=eds-live)  
1026 [live](https://search.ebscohost.com/login.aspx?direct=true&db=bth&AN=9793888&site=eds-live) (Accessed: October 2021).

1027 Gibb, A., Drake, C. and Jones, W. (2018) Costs of occupational ill - health in construction.  
1028 London: Institution of Civil Engineers. Available via:  
1029 [https://www.ice.org.uk/ICEDevelopmentWebPortal/media/Documents/ Disciplines%20an](https://www.ice.org.uk/ICEDevelopmentWebPortal/media/Documents/ Disciplines%20and%20Resources/Briefing%20Sheet/ Costs-of-occupational-ill-health-in-)  
1030 [d%20Resources/Briefing%20Sheet/ Costs-of-occupational-ill-health-in-](https://www.ice.org.uk/ICEDevelopmentWebPortal/media/Documents/ Disciplines%20and%20Resources/Briefing%20Sheet/ Costs-of-occupational-ill-health-in-)  
1031 [constructionformattedFINAL.pdf](https://www.ice.org.uk/ICEDevelopmentWebPortal/media/Documents/ Disciplines%20and%20Resources/Briefing%20Sheet/ Costs-of-occupational-ill-health-in-) (Accessed: August 2021).

1032 Goodrum, P. M., McLaren, M. A., and Durfee, A. (2006) The application of active radio frequency  
1033 identification technology for tool tracking on construction job sites. *Automation in*  
1034 *Construction*, Vol. 15, No. 3, pp. 292-302. DOI:  
1035 <https://doi.org/10.1016/j.autcon.2005.06.004>.

1036 Guo, H., Yu, Y., and Skitmore, M. (2017) Visualization technology-based construction safety  
1037 management: a review. *Automation in Construction*, Vol. 73, pp. 135–144. DOI:  
1038 <http://dx.doi.org/10.1016/j.autcon.2016.10.004>.

1039 Han, S., and Lee, S. (2013) A vision-based motion capture and recognition framework for  
1040 behavior-based safety management. *Automation in Construction*. Vol. 35, pp. 131–141.  
1041 DOI: <http://dx.doi.org/10.1016/j.autcon.2013.05.001>.

1042 Health and Safety Executive (HSE) (2020) Construction Statistics in Great Britain, 2020.  
1043 Available via: <https://www.hse.gov.uk/statistics/industry/construction.pdf>. (Accessed:  
1044 August 2021).

1045 Hignett, S., and McAtamney, L. (2000) Rapid entire body assessment (REBA). *Applied*  
1046 *Ergonomics*, Vol. 31, No. 2, pp. 201–205. DOI: [http://dx.doi.org/10.1016/S0003-6870](http://dx.doi.org/10.1016/S0003-6870(99)00039-3)  
1047 [\(99\)00039-3](http://dx.doi.org/10.1016/S0003-6870(99)00039-3).

1048 Hochreiter, S., and Schmidhuber, J. (1997) Long short-term memory. *Neural Computation*, Vol.  
1049 9, No. 8, pp. 1735-1780. DOI: <https://doi.org/10.1162/neco.1997.9.8.1735>.

1050 Ijjina, E. P., and Chalavadi, K. M. (2017) Human action recognition in RGB-D videos using  
1051 motion sequence information and deep learning. *Pattern Recognition*, Vol. 72, pp. 504-516.  
1052 DOI: <https://doi.org/10.1016/j.patcog.2017.07.013>.

1053 Inoue, M., Inoue, S., and Nishida, T. (2018) Deep recurrent neural network for mobile human  
1054 activity recognition with high throughput. *Artificial Life and Robotics*, Vol. 23, No. 2, pp.  
1055 173-185. DOI: <https://doi.org/10.1007/s10015-017-0422-x>.

1056 International Organization for Standardization (ISO) (2006) Ergonomics evaluation of static  
1057 working postures, ISO 11226: 2000, Geneva. Available via:  
1058 <https://www.evs.ee/products/iso-11226-2000> (Accessed: August 2021).

1059 Joshua, L., and Varghese, K. (2010) Accelerometer-based activity recognition in  
1060 construction. *Journal of Computing in Civil Engineering*, Vol. 25, No. 5, pp. 370-379. DOI:  
1061 [https://doi.org/10.1061/\(ASCE\)CP.1943-5487.0000097](https://doi.org/10.1061/(ASCE)CP.1943-5487.0000097).

1062 Karwowski, W. (2001) International encyclopedia of ergonomics and human factors, 2<sup>nd</sup> Edition,  
1063 Vol. 3, CRC Press, LLC. ISBN: 9780415304306.

1064 Kim, K., and Cho, Y. K. (2020) Effective inertial sensor quantity and locations on a body for deep  
1065 learning-based worker's motion recognition. *Automation in Construction*, Vol. 113, pp.  
1066 103126. DOI: <https://doi.org/10.1016/j.autcon.2020.103126>.

1067 Kingma, D. P., and Ba, J. (2014) Adam: A method for stochastic optimization. *arXiv preprint*  
1068 *arXiv:1412.6980*. Available via: <http://arxiv.org/abs/1412.6980> (Accessed: October 2021).

1069 Kivi, P., and Mattila, M. (1991) Analysis and improvement of work postures in the building  
1070 industry: application of the computerised OWAS method. *Applied Ergonomics*, Vol. 22,  
1071 No. 1, pp. 43–48. DOI: [https://doi.org/10.1016/0003-6870\(91\)90009-7](https://doi.org/10.1016/0003-6870(91)90009-7).

1072 Lee, H., Yang, K., Kim, N., and Ahn, C. R. (2020) Detecting excessive load-carrying tasks using  
1073 a deep learning network with a Gramian Angular Field. *Automation in Construction*, Vol.  
1074 120, pp. 103390. DOI: <https://doi.org/10.1016/j.autcon.2020.103390>.

1075 Lee, J., Joo, H., Lee, J., and Chee, Y. (2020) Automatic classification of squat posture using inertial  
1076 sensors: Deep learning approach. *Sensors*, Vol. 20, No. 2, pp. 361. DOI:  
1077 <https://doi.org/10.3390/s20020361>.

1078 Li, H., Shrestha, A., Heidari, H., Le Kernec, J., and Fioranelli, F. (2019). Bi-LSTM network for  
1079 multimodal continuous human activity recognition and fall detection. *IEEE Sensors*  
1080 *Journal*, Vol. 20, No. 3, pp. 1191-1201. DOI: <https://doi.org/10.1109/JSEN.2019.2946095>.

1081 Mantyjarvi, J., Himberg, J., and Seppanen, T. (2001) Recognizing human motion with multiple  
1082 acceleration sensors. In 2001 IEEE International Conference on Systems, Man and  
1083 Cybernetics. E-systems and E-man for Cybernetics in Cyberspace (cat. no. 01ch37236),  
1084 Vol. 2, pp. 747-752. DOI: <https://doi.org/10.1109/ICSMC.2001.973004>.

1085 Mcatamney, L., and Corlett, N. E. (1993) RULA: A survey method for the investigation of work-  
1086 related upper limb disorders. *Applied Ergonomics*, Vol. 24, No. 2, pp. 91–99. DOI:  
1087 [http://dx.doi.org/10.1016/0003-6870\(93\)90080-S](http://dx.doi.org/10.1016/0003-6870(93)90080-S).

1088 Mekruksavanich, S., and Jitpattanakul, A. (2021) LSTM networks using smartphone data for  
1089 sensor-based human activity recognition in smart homes. *Sensors*, Vol. 21, No. 5, pp. 1636.  
1090 DOI: <https://doi.org/10.3390/s21051636>.

1091 Nath, N. D., Chaspari, T., and Behzadan, A. H. (2018) Automated ergonomic risk monitoring  
1092 using body-mounted sensors and machine learning. *Advanced Engineering*  
1093 *Informatics*, Vol. 38, pp. 514-526. DOI: <https://doi.org/10.1016/j.aei.2018.08.020>.



- 1094 Nguyen, T. N., Lee, S., Nguyen-Xuan, H., and Lee, J. (2019) A novel analysis-prediction approach  
 1095 for geometrically nonlinear problems using group method of data handling. *Computer*  
 1096 *Methods in Applied Mechanics and Engineering*, Vol. 354, pp. 506-526. DOI:  
 1097 <https://doi.org/10.1016/j.cma.2019.05.052>.
- 1098 Ordóñez, F. J., and Roggen, D. (2016) Deep convolutional and LSTM recurrent neural networks  
 1099 for multimodal wearable activity recognition. *Sensors*, Vol. 16, No. 1, pp. 115. DOI:  
 1100 <https://doi.org/10.3390/s16010115>.
- 1101 Portugal, I., Alencar, P., and Cowan, D. (2018) The use of machine learning algorithms in  
 1102 recommender systems: A systematic review. *Expert Systems with Applications*, Vol. 97,  
 1103 pp. 205-227. DOI: <https://doi.org/10.1016/j.eswa.2017.12.020>.
- 1104 Preece, S. J., Goulermas, J. Y., Kenney, L. P., Howard, D., Meijer, K., and Crompton, R. (2009)  
 1105 Activity identification using body-mounted sensors—a review of classification  
 1106 techniques. *Physiological Measurement*, Vol. 30, No. 4, R1–R33. DOI:  
 1107 <https://doi.org/10.1088/0967-3334/30/4/R01>.
- 1108 Rashid, K. M., and Louis, J. (2019) Times-series data augmentation and deep learning for  
 1109 construction equipment activity recognition. *Advanced Engineering Informatics*, Vol. 42,  
 1110 pp. 100944. DOI: <https://doi.org/10.1016/j.aei.2019.100944>.
- 1111 Ray, S. J., and Teizer, J. (2012) Real-time construction worker posture analysis for ergonomics  
 1112 training. *Advanced Engineering Informatics*, Vol. 26, No. 2, pp. 439–455. DOI:  
 1113 <http://dx.doi.org/10.1016/j.aei.2012.02.011>.
- 1114 Ryu, J., Seo, J., Jebelli, H., and Lee, S. (2019) Automated action recognition using an  
 1115 accelerometer-embedded wristband-type activity tracker. *Journal of Construction*  
 1116 *Engineering and Management*, Vol. 145, No. 1, pp. 04018114. DOI:  
 1117 [https://doi.org/10.1061/\(ASCE\)CO.1943-7862.0001579](https://doi.org/10.1061/(ASCE)CO.1943-7862.0001579).
- 1118 Safe Work Australia. (2020) Key work health and safety statistics Australia 2020: Work-related  
 1119 injury fatalities. Available at:  
 1120 [https://www.safeworkaustralia.gov.au/sites/default/files/2020-](https://www.safeworkaustralia.gov.au/sites/default/files/2020-11/Key%20Work%20Health%20and%20Safety%20Stats%202020.pdf)  
 1121 [11/Key%20Work%20Health%20and%20Safety%20Stats%202020.pdf](https://www.safeworkaustralia.gov.au/sites/default/files/2020-11/Key%20Work%20Health%20and%20Safety%20Stats%202020.pdf). (Accessed:  
 1122 August 2021).
- 1123 Seo, J., and Lee, S. (2021) Automated postural ergonomic risk assessment using vision-based  
 1124 posture classification. *Automation in Construction*, Vol. 128, pp. 103725. DOI:  
 1125 <https://doi.org/10.1016/j.autcon.2021.103725>.
- 1126 Seo, J., Starbuck, R., Han, S., Lee, S., and Armstrong, T. J. (2015) Motion data-driven  
 1127 biomechanical analysis during construction tasks on sites. *Journal of Computing in Civil*  
 1128 *Engineering*, Vol. 29, No. 4, pp. B4014005. DOI:  
 1129 [https://doi.org/10.1061/\(ASCE\)CP.1943-5487.0000400](https://doi.org/10.1061/(ASCE)CP.1943-5487.0000400).
- 1130 Seyfioglu, M. S., Özbayoğlu, A. M., and Gürbüz, S. Z. (2018) Deep convolutional autoencoder  
 1131 for radar-based classification of similar aided and unaided human activities. *IEEE*  
 1132 *Transactions on Aerospace and Electronic Systems*, Vol. 54, No. 4, pp. 1709-1723. DOI:  
 1133 <https://doi.org/10.1109/TAES.2018.2799758>.
- 1134 Son, H., Choi, H., Seong, H., and Kim, C. (2019) Detection of construction workers under varying  
 1135 poses and changing background in image sequences via very deep residual  
 1136 networks. *Automation in Construction*, Vol. 99, pp. 27-38. DOI:  
 1137 <https://doi.org/10.1016/j.autcon.2018.11.033>.
- 1138 Srivastava, N., Hinton, G., Krizhevsky, A., Sutskever, I., and Salakhutdinov, R. (2014) Dropout:  
 1139 a simple way to prevent neural networks from overfitting. *The Journal of Machine*

1140 Learning Research, Vol. 15, No. 1, pp. 1929-1958. Available via:  
1141 <http://jmlr.org/papers/v15/srivastava14a.html> (Accessed: October 2021).

1142 Teizer, J., Caldas, C. H., and Haas, C. T. (2007) Real-time three-dimensional occupancy grid  
1143 modeling for the detection and tracking of construction resources. *Journal of Construction*  
1144 *Engineering and Management*, Vol. 133, No. 11, pp. 880-888. DOI:  
1145 [https://doi.org/10.1061/\(ASCE\)0733-9364\(2007\)133:11\(880\)](https://doi.org/10.1061/(ASCE)0733-9364(2007)133:11(880)).

1146 Umer, W., Antwi-Afari, M. F., Li, H., Szeto, G. P., and Wong, A. Y. L. (2017a) The prevalence  
1147 of musculoskeletal symptoms in the construction industry: A systematic review and meta-  
1148 analysis. *International Archives of Occupational and Environmental Health*, Vol. 91, No.  
1149 2, pp. 125-144. DOI: <https://doi.org/10.1007/s00420-017-1273-4>.

1150 Umer, W., Li, H., Szeto, G. P. Y., and Wong, A. Y. L. (2017b) Identification of biomechanical  
1151 risk factors for the development of lower-back disorders during manual rebar tying. *Journal*  
1152 *of Construction Engineering and Management*, Vol. 143, No. 1, pp. 04016080. DOI:  
1153 [https://doi.org/10.1061/\(ASCE\)CO.1943-7862.0001208](https://doi.org/10.1061/(ASCE)CO.1943-7862.0001208).

1154 Umer, W., Li, H., Yu, Y., Antwi-Afari, M. F., Anwer, S., and Luo, X. (2020) Physical exertion  
1155 modeling for construction tasks using combined cardiorespiratory and thermoregulatory  
1156 measures. *Automation in Construction*, Vol. 112, pp. 103079. DOI:  
1157 <https://doi.org/10.1016/j.autcon.2020.103079>.

1158 Valero, E., Sivanathan, A., Bosché, F., and Abdel-Wahab, M. (2017) Analysis of construction  
1159 trade worker body motions using a wearable and wireless motion sensor  
1160 network. *Automation in Construction*, Vol. 83, pp. 48-55. DOI:  
1161 <https://doi.org/10.1016/j.autcon.2017.08.001>.

1162 Wang, D., Dai, F., and Ning, X. (2015a) Risk assessment of work-related musculoskeletal  
1163 disorders in construction: state-of-the-art review. *Journal of Construction Engineering and*  
1164 *Management*, Vol. 141, No. 6, pp. 1–15. DOI: [http://dx.doi.org/10.1061/\(ASCE\)CO.1943-7862.0000979](http://dx.doi.org/10.1061/(ASCE)CO.1943-7862.0000979).

1166 Wang, J., Chen, D., Zhu, M., and Sun, Y. (2021). Risk assessment for musculoskeletal disorders  
1167 based on the characteristics of work posture. *Automation in Construction*, Vol. 131, pp.  
1168 103921. DOI: <https://doi.org/10.1016/j.autcon.2021.103921>.

1169 Xing, X., Zhong, B., Luo, H., Rose, T., Li, J., and Antwi-Afari, M. F. (2020) Effects of physical  
1170 fatigue on the induction of mental fatigue of construction workers: A pilot study based on  
1171 a neurophysiological approach. *Automation in Construction*, Vol. 120, pp. 103381. DOI:  
1172 <https://doi.org/10.1016/j.autcon.2020.103381>.

1173 Yan, X., Li, H., Li, A. R., and Zhang, H. (2017) Wearable IMU-based real-time motion warning  
1174 system for construction workers' musculoskeletal disorders prevention. *Automation in*  
1175 *Construction*, Vol. 74, pp. 2-11. DOI: <https://doi.org/10.1016/j.autcon.2016.11.007>.

1176 Yang, K., Ahn, C. R., and Kim, H. (2020) Deep learning-based classification of work-related  
1177 physical load levels in construction. *Advanced Engineering Informatics*, Vol. 45, pp.  
1178 101104. DOI: <https://doi.org/10.1016/j.aei.2020.101104>.

1179 Yang, S., Yu, X., and Zhou, Y. (2020) LSTM and GRU neural network performance comparison  
1180 study: Taking Yelp review dataset as an example. In *2020 International Workshop on*  
1181 *Electronic Communication and Artificial Intelligence (IWEC AI)*, pp. 98-101. DOI:  
1182 <https://doi.org/10.1109/IWEC AI50956.2020.00027>.

1183 Yang, X., Li, H., Yu, Y., Luo, X., Huang, T., and Yang, X. (2018) Automatic pixel-level crack  
1184 detection and measurement using fully convolutional network. *Computer-Aided Civil and*

1185 Infrastructure Engineering, Vol. 33, No. 12, pp. 1090-1109. DOI:  
1186 <https://doi.org/10.1111/mice.12412>.

1187 Yilmaz, A., Javed, O., and Shah, M. (2006) Object tracking: A survey. *ACM Computing Surveys*  
1188 (CSUR), Vol. 38, No. 4, pp. 13-es. DOI: <https://doi.org/10.1145/1177352.1177355>.

1189 Yu, Y., Umer, W., Yang, X., and Antwi-Afari, M. F. (2021) Posture-related data collection  
1190 methods for construction workers: A review. *Automation in Construction*, Vol. 124, pp.  
1191 103538. DOI: <https://doi.org/10.1016/j.autcon.2020.103538>.

1192 Yu, Y., Yang, X., Li, H., Luo, X., Guo, H., and Fang, Q. (2019) Joint-level vision-based ergonomic  
1193 assessment tool for construction workers. *Journal of Construction Engineering and*  
1194 *Management*, Vol. 145, No. 5, pp. 04019025. DOI:  
1195 [https://doi.org/10.1061/\(ASCE\)CO.1943-7862.0001647](https://doi.org/10.1061/(ASCE)CO.1943-7862.0001647).

1196 Zarzycki, K., and Ławryńczuk, M. (2021) LSTM and GRU neural networks as models of  
1197 dynamical processes used in predictive control: A comparison of models developed for two  
1198 chemical reactors. *Sensors*, Vol. 21, No. 16, pp. 5625. DOI:  
1199 <https://doi.org/10.3390/s21165625>.

1200 Zhang, H., Yan, X., and Li, H. (2018) Ergonomic posture recognition using 3D view-invariant  
1201 features from single ordinary camera. *Automation in Construction*, Vol. 94, pp. 1-10. DOI:  
1202 <https://doi.org/10.1016/j.autcon.2018.05.033>.

1203 Zhao, J., and Obonyo, E. (2020) Convolutional long short-term memory model for recognizing  
1204 construction workers' postures from wearable inertial measurement units. *Advanced*  
1205 *Engineering Informatics*, Vol. 46, pp. 101177. DOI:  
1206 <https://doi.org/10.1016/j.aei.2020.101177>.

1207 Zhao, J., and Obonyo, E. (2021) Applying incremental Deep Neural Networks-based posture  
1208 recognition model for ergonomics risk assessment in construction. *Advanced Engineering*  
1209 *Informatics*, Vol. 50, pp. 101374. DOI: <https://doi.org/10.1016/j.aei.2021.101374>.

1210 Zhong, B., Li, H., Luo, H., Zhou, J., Fang, W., and Xing, X. (2020) Ontology-based semantic  
1211 modeling of knowledge in construction: classification and identification of hazards implied  
1212 in images. *Journal of Construction Engineering and Management*, Vol. 146, No. 4, pp.  
1213 04020013. DOI: [https://doi.org/10.1061/\(ASCE\)CO.1943-7862.0001767](https://doi.org/10.1061/(ASCE)CO.1943-7862.0001767).

1214 Zhong, B., Xing, X., Luo, H., Zhou, Q., Li, H., Rose, T., and Fang, W. (2020) Deep learning-based  
1215 extraction of construction procedural constraints from construction regulations. *Advanced*  
1216 *Engineering Informatics*, Vol. 43, pp. 101003. DOI:  
1217 <https://doi.org/10.1016/j.aei.2019.101003>.